catalysts

MDPI

Review

Strategies to Enhance the Catalytic Performance of ZSM-5 Zeolite in Hydrocarbon Cracking: A Review

Yajun Ji, Honghui Yang * and Wei Yan *

The State Key Laboratory of Multiphase Flow in Power Engineering, Department of Environmental Science and Engineering, Xi'an Jiaotong University, Xi'an 710049, China; jiyajun928@stu.xjtu.edu.cn

* Correspondence: yanghonghui@xjtu.edu.cn (H.Y.); yanwei@xjtu.edu.cn (W.Y.); Tel.: +86-29-8266-9033 (H.Y. & W.Y.)

Received: 30 October 2017; Accepted: 21 November 2017; Published: 29 November 2017

Abstract: ZSM-5 zeolite is widely used in catalytic cracking of hydrocarbon, but the conventional ZSM-5 zeolite deactivates quickly due to its simple microporous and long diffusion pathway. Many studies have been done to overcome these disadvantages recently. In this review, four main approaches for enhancing the catalytic performance, namely synthesis of ZSM-5 zeolite with special morphology, hierarchical ZSM-5 zeolite, nano-sized ZSM-5 zeolite and optimization of acid properties, are discussed. ZSM-5 with special morphology such as hollow, composite and nanosheet structure can effectively increase the diffusion efficiency and accessibility of acid sites, giving high catalytic activity. The accessibility of acid sites and diffusion efficiency can also be enhanced by introducing additional mesopores or macropores. By decreasing the crystal size to nanoscale, the diffusion length can be shortened. The catalytic activity increases and the amount of carbon deposition decreases with the decrease of crystal size. By regulating the acid properties of ZSM-5 with element or compound modification, the overreaction of reactants and formation of carbon deposition could be suppressed, thus enhancing the catalytic activity and light alkene selectivity. Besides, some future needs and perspectives of ZSM-5 with excellent cracking activity are addressed for researchers' consideration.

Keywords: ZSM-5 zeolite; hydrocarbon; catalytic cracking; morphology; hierarchical zeolite; nano-sized zeolite; acid property

1. Introduction

Zeolites are crystalline aluminosilicate fabricated by silica tetrahedron and alumina tetrahedron through oxygen bridges. They are widely applied in petrochemical chemistry [1,2], environmental protection [3,4] and adsorption [5] because of high BET (Brunauer-Emmett-Teller) surface area, special channel structure, abundant acid sites, and thermal and hydrothermal stability [6]. Catalytic cracking of hydrocarbon is significant for industrial manufacture, due to the advantages of high cracking conversion efficiency, high light alkene selectivity and less carbon deposition compared with thermal cracking [7]. Among the catalysts for hydrocarbon catalytic cracking, ZSM-5 zeolite is the most widely used due to its particular advantages of its acidity, special pore structure, and high thermal and hydrothermal stability [8,9]. When it was applied in *n*-hexane cracking under high pressure, it showed better catalytic activity and stability, higher light alkene selectivity and less sensitivity to deactivation by carbon deposition than H-MOR, H-BEA and USY zeolites [10].

The conventional ZSM-5 zeolite, however, is also easily deactivated by carbon deposition because of its simple microporous structure, long diffusion pathway and redundant strong acid sites. Although strong acid sites are crucial for catalytic reactions, especially for hydrocarbon cracking, the reactants would over-react on the acid sites and convert to aromatic hydrocarbons or carbon deposition if too many acid sites exist, resulting in the deactivation of catalyst. Moreover, as only microporous structure exists in conventional ZSM-5 zeolite, the diffusion efficiency of molecule is

low. Large molecules are difficult to diffuse in micropores. They finally turn into carbon deposition, blocking the pore channel. The diffusion pathway length in conventional ZSM-5 zeolite is too long, which hinders the diffusion of molecule resulting in a low catalytic activity.

Therefore, many studies have been conducted to overcome these limitations, such as preparation of zeolite with special morphology [11,12], hierarchical zeolite [13,14] or nano-sized zeolite [15], and element or compound modification [16]. Ryoo et al. [12] firstly prepared the nanosheet MFI zeolite in 2009. This nanosheet zeolite contained both microporous and mesoporous structure, which enhanced the diffusion of reactants. Besides, the nanosheets were very thin, which reduced the diffusion lengths and improved the catalytic activity further. It showed higher catalytic conversion of bulky molecules than conventional ZSM-5 zeolite. In addition, the hierarchical ZSM-5 zeolite was synthesized by adding soluble starch, sodium carboxymethyl cellulose [17] or anion exchange resin [18] as a second mesoporous template, and their catalytic activities were promoted with the increasing of mesopores by improving the diffusion efficiency and accessibility of acid sites.

Overall, it can be summarized that the catalytic performance of ZSM-5 zeolite can be influenced by its pore channel structure, diffusion pathway length, acid amount and acid strength. Herein, we have reviewed the pioneered studies and recent developments about how to enhance the catalytic performance of ZSM-5 zeolite in catalytic cracking of hydrocarbons from the following aspects:

(1) Synthesis of ZSM-5 zeolite with special morphology to decrease the diffusion pathway or increase the diffusion efficiency;
(2) Synthesis of hierarchical ZSM-5 zeolite with extra mesopores or macropores to increase the diffusion efficiency of molecules and the accessibility of acid sites;
(3) Synthesis of nano-sized ZSM-5 zeolite with short diffusion length to promote the diffusion of molecules and;
(4) Optimization of the acid properties of ZSM-5 zeolite to enhance the catalytic activity.

For each of these strategies, its advantages and limitations are discussed and compared with each other from the aspects of synthesis process, catalytic activity and potential for industrial application.

2. ZSM-5 Zeolite with Special Morphology

ZSM-5 zeolites with special morphology are designed in order to decrease the diffusion length or enhance the diffusion efficiency, such as hollow ZSM-5 zeolite, nanosheet MFI zeolite, *b*-oriented MFI zeolite, nanorod-oriented zeolite, composite zeolite and fiber-sized zeolite and so on. When the diffusion length decreases or the diffusion efficiency increases, reactant and product could transform quickly to and away from the acid sites within the zeolite crystals and, thus, shift the selectivity to favor the production of more valuable products at reduced yields of coke [19].

2.1. Hollow ZSM-5 Zeolite

In hollow ZSM-5 zeolite with thin shell, the diffusion pathway can be reduced effectively compared with the conventional bulk ZSM-5 zeolite duo to its excellent textural properties (Table 1) resulting from the hollow voids in zeolite crystals. It has been proven that hollow ZSM-5 zeolite showed improved catalytic activity in hydrocarbon cracking by enhancing the diffusion of molecules [20]. It can be prepared by hard/soft-template method or selectively dissolving the inner part of zeolite crystals.

Table 1. Textural properties of ZSM-5 zeolite with special morphology in the references.

Sample	S_{BET} [a] ($m^2 \cdot g^{-1}$)	S_{ext} [b] ($m^2 \cdot g^{-1}$)	V_{Tot} [c] ($cm^3 \cdot g^{-1}$)	V_{mic} [d] ($cm^3 \cdot g^{-1}$)	V_{mes} [e] ($cm^3 \cdot g^{-1}$)	R [f]
Z50_10 h	383	71	0.37	0.15	0.22	[21]
Hollow ZSM-5	443	105	0.74	0.15	0.59	[22]
H-ZSM-5/MCM-41	548	-	0.49	0.10	0.39	[23]
HZM-N(50)	562	256	0.80	0.34	0.46	[24]
50L-1st	918	-	0.94	-	-	[25]
50L-2nd	913	-	0.94	-	-	[25]
HZ-ER	572	-	0.40	0.05	0.35	[26]
$MZ_{AT0.2\text{-}PI0.02}$@MSA	539	358	0.61	0.09	0.52	[27]
ZSM-5@SAPO-34(6)	474	148	0.48	0.13	0.35	[28]
ZSC-24	361	233	0.84	0.06	0.78	[29]

[a] BET surface area; [b] External surface area; [c] Total volume; [d] Micropore volume; [e] Mesopore volume; [f] Reference.

For hard-template method, polystyrene microsphere and carbon black are widely used as the core to prepare hollow zeolite. However, as large amounts of templates are necessary to serve as the core, it is costly and environmentally unfriendly for industrial application to remove these hard templates by burning under air atmosphere and high temperature. For soft-template method, fewer templates are needed to induce the generation of hollow zeolite compared with hard-template method. Jiang et al. [30] prepared hollow ZSM-5 crystals through hydrothermal crystallization method in the presence of polyacrylamide (PAM) as the soft template under the condition of low crystallization temperature (120 °C) and high PAM concentration. Wang et al. [31] synthesized the hollow microsphere ZSM-5 zeolite through a dissolution–recrystallization procedure with the assistance of organosilanes. The amorphous spherical was formed at 140 °C in 12 h firstly in the presence of organosilanes. Then, nanocrystals were generated when the crystallization time was prolonged to 48 h, and they self-assembled on the external surface of the microspheres to form the core/shell structure. Finally, the synthesis gel was recrystallized at 120 °C for 72 h. At this temperature, the dissolution rate was higher than the crystallization rate, resulting in hollow structure. The dissolved fragments further recrystallized into the zeolite framework of nanocrystals (Figure 1). Pashkova et al. [32] synthesized hollow ZSM-5 zeolite by self-templating process without the addition of hard or soft template for sphere formation or structure-directing agent for zeolite nucleation. By spray-drying the colloidal solution of silicic acid and aluminum butoxide, the pre-shaped aluminosilicate precursor was obtained, which could act as both the shape-directing agent and source of silica and alumina for zeolite formation. The self-templating process for hollow ZSM-5 zeolite preparation is instructive to design zeolite with different morphology.

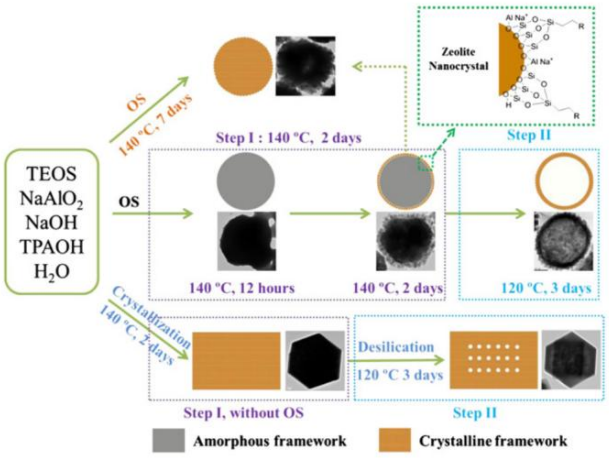

Figure 1. Schematic illustration of the structural changes of hollow zeolite spheres during crystallization procedure [31]. Copyright Elsevier, 2013.

Another route to prepare hollow ZSM-5 zeolite is to selectively dissolve silicon components with alkali solution. When ZSM-5 zeolite is prepared with the assistance of organic structure-directing agent, the aluminum and silicon distribute heterogeneously, with aluminum rich surface and silicon rich core. Thus, the silicon rich core is preferentially dissolved by alkali solution to generate hollow structure. Hollow structural ZSM-5 zeolite was obtained by sodium hydroxide solution treatment by Groen et al. [33]. The shell of this hollow ZSM-5 zeolite was heterogeneous due to the non-uniformity of the precursor and/or the severe dissolution of the zeolite crystals by the sodium hydroxide solution. When the crystal size of ZSM-5 zeolite was below 100 nm, it was feasible to obtain hollow zeolite with uniform shell thickness [21]. Xie et al. [20] prepared the regular ZSM-5 microboxes through sodium carbonate treatment, which was a milder method than sodium hydroxide treatment. Guo et al. [22] prepared hollow ZSM-5 single crystals by hydrothermal treatment in tetrapropylammonium hydroxide solution (TPAOH). The silicon in the interior of the zeolite was selectively dissolved and recrystallized on the exterior. They also proved that this post-treatment method was only effective on zeolites with Si/Al ratio ranged from 40 to 74 and the nanocrystal size ranged from 150 to 330 nm (Figure 2). It indicated that the selective dissolution of silicon components was limited to specific Si/Al ratio and nano-sized zeolites. Besides, it was wasteful in industrial application, because much aluminosilicate was dissolved.

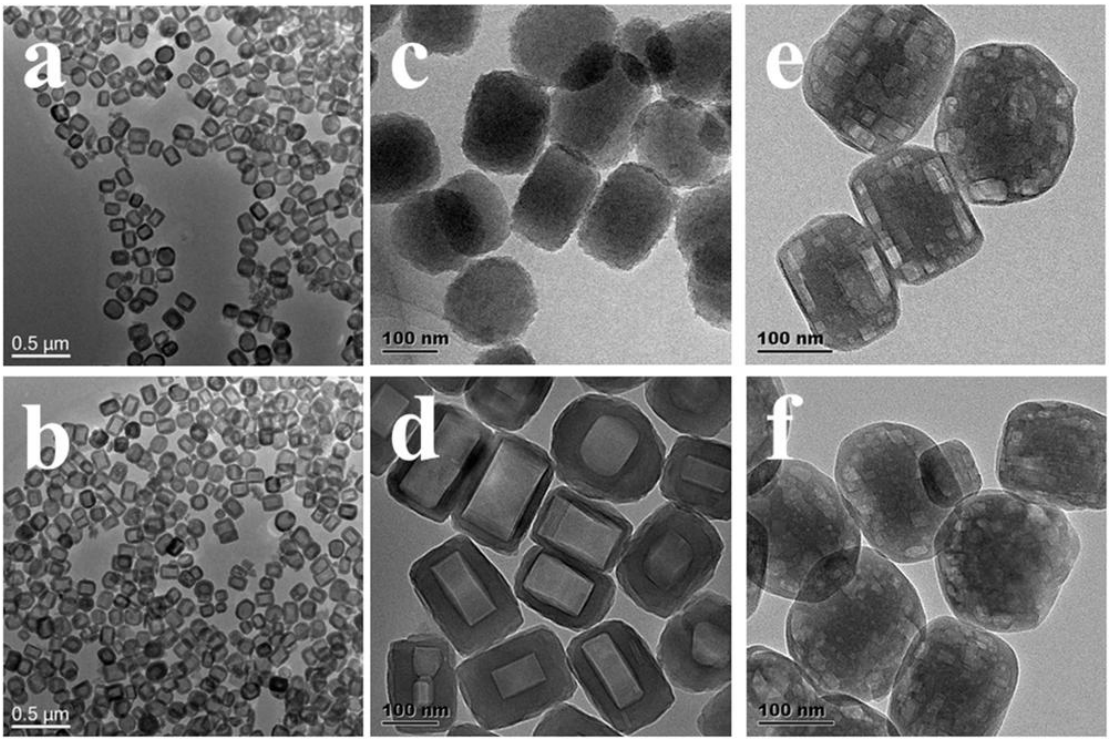

Figure 2. TEM images of ZSM-5 with different parent Si/Al ratios after TPAOH treatment at 170 °C for 72 h. (**a**,**b**) The parent Si/Al ratio is 40, and the concentrations of TPAOH are 0.1 and 0.2 M, respectively. (**c**,**d**) The parent Si/Al ratio is 59, and the concentrations of TPAOH are 0.1 and 0.2 M, respectively. (**e**,**f**) The parent Si/Al ratio is 79, and the concentrations of TPAOH are 0.2 and 0.5 M, respectively [22]. Copyright Wiley-VCH Verlag GmbH and Co., 2015.

2.2. Zeolitic Composites of ZSM-5 and Other Materials

As only micropores exist and the diffusion pathway is too long for the conventional ZSM-5 zeolite, many studies focused on synthesis of composite zeolites using ZSM-5 zeolite as the functional component to enhance the catalytic cracking activity, such as ZSM-5@MCM-41, ZSM-5@SBA-15, ZSM-5@SAPO-34, ZSM-5@KIT-1 and so on. The composite zeolites not only maintained the intrinsic activity of ZSM-5 zeolite, but also showed synergistic effect with other materials. For catalytic cracking

of hydrocarbon, a second zeolite was usually introduced to increase the diffusion of molecule and the accessibility of acid sites in the micropores of ZSM-5 zeolite, thus enhancing the catalytic activity of ZSM-5 zeolite [34].

ZSM-5@MCM-41 composite zeolite was prepared by treating ZSM-5 zeolite with sodium hydroxide solution, and then the dissolved silica and aluminum were recrystallized on the surface of ZSM-5 zeolites in the form of MCM-41 in the presence of cetyltrimethylammonium bromide (CTAB) [23–25,35]. After addition of MCM-41, ZSM-5@MCM-41 composite exhibited more appropriate acid distribution and strength, shorter pathway length and higher external surface area. The conversion of *n*-decane cracking increased from 61.7 to 93.0% and it maintained at 89.3% after reaction for 170 min, while that of the parent ZSM-5 was just 56.4% [24]. When it was applied in *n*-dodecane cracking, the conversion increased by 25% and it kept a stable activity within 30 min [35]. Wang et al. [25] studied the influence of alkali concentration, dissolution temperature, dissolution time and CTAB concentration on the synthesis of ZSM-5-based mesostructures in laboratory scale. Above all, they expanded the scale from 0.25 L to 5 and 50 L. The obtained products exhibited excellent textural properties, which were of significant importance for industrial application. During the preparation process, a proper amount of CTAB was necessary to generate the MCM-41 shell. A high concentration of CTAB would cause the recrystallization of ZSM-5 zeolite and restrain the formation of hexagonal phase of mesoporous materials MCM-41 [36]. Liu et al. [26] prepared the meso-HZSM-5@Al-MCM-41 zeolite by dissolving the parent ZSM-5 zeolite to generate the meso-ZSM-5 zeolite with tetramethylammonium hydroxide (TMAOH) or tetraethylammonium hydroxide (TEAOH) firstly. Then, the aluminosilicate fragments recrystallized with the assistance of CTAB on the external surface of ZSM-5 zeolite to form this meso-HZSM-5@Al-MCM-41 zeolite. During the catalytic cracking of *n*-dodecane, the conversion rate increased by 30% and it showed more stable catalytic activity than ZSM-5 zeolite. It was explained that the MCM-41 shell enhanced the accessibility of acid sites and diffusion efficiency of molecule due to the shorter pathway and ordered mesoporous structure, as well as the pre-cracking of reactants in the MCM-41 shell (Figure 3). Besides, this method avoided the ion exchange with NH_4NO_3 and calcining processes to obtain protonated zeolite compared with NaOH treatment method.

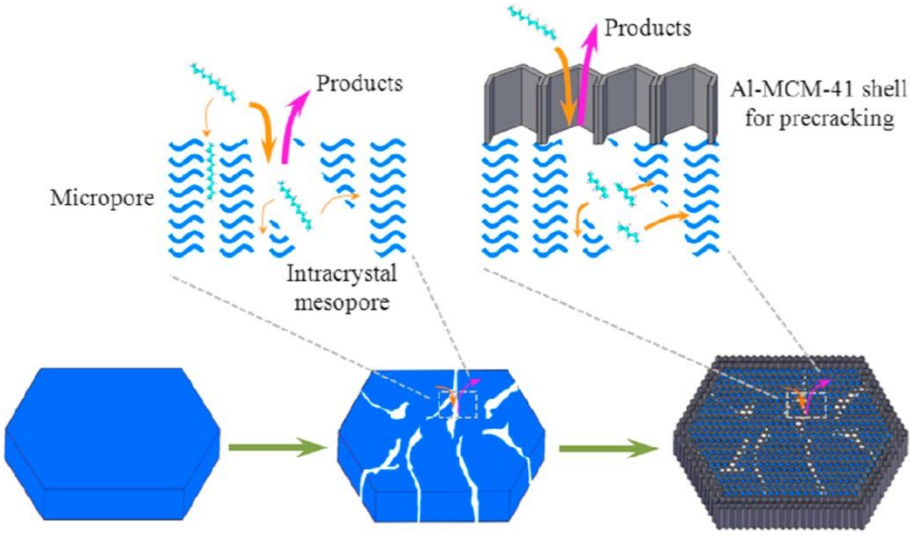

Figure 3. A schematic diagram of catalytic cracking of hydrocarbon over meso-HZSM-5@Al-MCM-41 zeolite [26]. Copyright Elsevier, 2015.

Similarly, Wu et al. [27] prepared a series of core–shell structured zeolitic composite with ZSM-5 as core and mesoporous aluminosilicate as shell by a dissolution and self-assembly method. The core–shell structured zeolite effectively reduced the diffusion length. Besides, the mesoporous shell could function as a supporter for Pt nano particles which led to a bifunctional catalyst for catalytic

cracking reactions. It showed higher conversion of 80.4% and high selectivity toward C_5–C_{11} of 58% for *n*-hexadecane cracking. ZSM-5@SAPO-34 zeolite with hierarchical pore sizes between 15 and 150 nm was prepared by partially dissolving the conventional ZSM-5 zeolite, and the acidity properties could be adjusted by varying the mass of ZSM-5 in the ZSM-5@SAPO-34, leading to higher catalytic performance than that of the parent ZSM-5 zeolite [28].

Li et al. [37] prepared the ZSM-5@KIT-1 composite zeolite with larger BET surface area and mesopore volume by adding ionic liquid as the mesoporous template during the conventional synthesis process. The precursor zeolite colloidal species were aged for different periods, followed by adding 1-hexadecyl-3- methylimidazolium bromide as the mesoporous template to form KIT-1 crystals around the surface of ZSM-5 crystals. Besides, the proportion of ZSM-5 zeolite and KIT-1 can be controlled facilely by varying the pre-aging time.

ZSM-5@silicalite-1 zeolite was prepared by adding silicalite-1 as the shell. The surface acidity of ZSM-5 zeolite could be deactivated after adding silicalite-1 shell. It restrained the carbon depositing on the external surface, which avoided the decreasing accessibility of acid site in the pore channel. Overall, ZSM-5@silicalite-1 with passivated surface acid sites could enhance the catalytic stability and product selectivity without sacrificing its catalyst activity [38,39].

Vu et al. [40] prepared the nanosized-ZSM-5@SBA-15 composites through a two-step process. They firstly obtained the partially crystalline ZSM-5 crystals by pre-crystallization for certain time. Then the unreacted precursors are converted to ordered mesoporous SBA-15 by adding surfactant solution and followed by hydrothermal treatment at 200 °C for 24 h. The ZSM-5@SBA-15 zeolite exhibited superior catalytic activity due to its medium acid sites, improved molecular transport efficiency resulting from the hierarchical pore structure and good hydrothermal stability. This special morphology effectively suppressed the secondary reactions among primarily generated light alkenes, thus providing higher light alkene selectivity (93.2%) in the catalytic cracking of triglyceride-rich biomass [29,40].

2.3. Nanosheet MFI Zeolite

The nanosheet MFI zeolite has the feature of hierarchical pore structure and thin lamellar structure, which overcomes the defects of simple microporous and long diffusion pathway in conventional ZSM-5 zeolite simultaneously. In 2009, Ryoo et al. [12] successfully prepared the nanosheet MFI zeolite by using a long-chain diquaternary ammonium-type surfactant ($C_{22}H_{45}$-$N^+(CH_3)_2$-C_6H_{12}-$N^+(CH_3)_2$-C_6H_{13}, designated $C_{22\text{-}6\text{-}6}$ hereafter) as the structure-directing agent (SDA). It showed higher and more stable catalytic cracking activity with less carbon deposition, even for large molecule. Thus, the nanosheet MFI zeolite has drawn much attention since then.

Inspired by this conception, Hensen et al. [41] prepared highly acidic nanosheet ZSM-5 zeolite by replacing the hexyl end group with propyl of SDA. The crystallization rate increased because of the higher occupancy of the intersections of the MFI framework by propyl than that of hexyl. Its lifetime was nearly two times as high as the conventional ZSM-5 zeolite. Xu et al. [42] designed a single quaternary ammonium head amphiphilic template by introducing bi-quaternary ammonium head groups and biphenyl groups into the SDA ((C_6H_{13}-$N^+(CH_3)_2$-C_6H_{12}-$N^+(CH_3)_2$-$(CH_2)_n$-O-C_6H_4-C_6H_4-O-$(CH_2)_n$-$N^+(CH_3)_2$-$N^+(CH_3)_2$-C_6H_{13}($4Br^-$), designated $BC_{Ph\text{-}n\text{-}6\text{-}6}$ hereafter). It exhibited strong ordered self-assembling ability through π-π stacking in hydrophobic side, which induced the formation of single crystalline mesostructured nanosheet zeolite (Figure 4). Besides, the length of alkyl spacers between two charged nitrogen cations in SDA strongly affected the morphology of the final catalyst. Only Pr6-diquat-5 could induce the formation of sequentially inter-grown MFI zeolite due to its molecular dimension and stabilization energy, which resulted in the unusual fitting of Pr6-diquat-5 inside the channels of MFI zeolite [43].

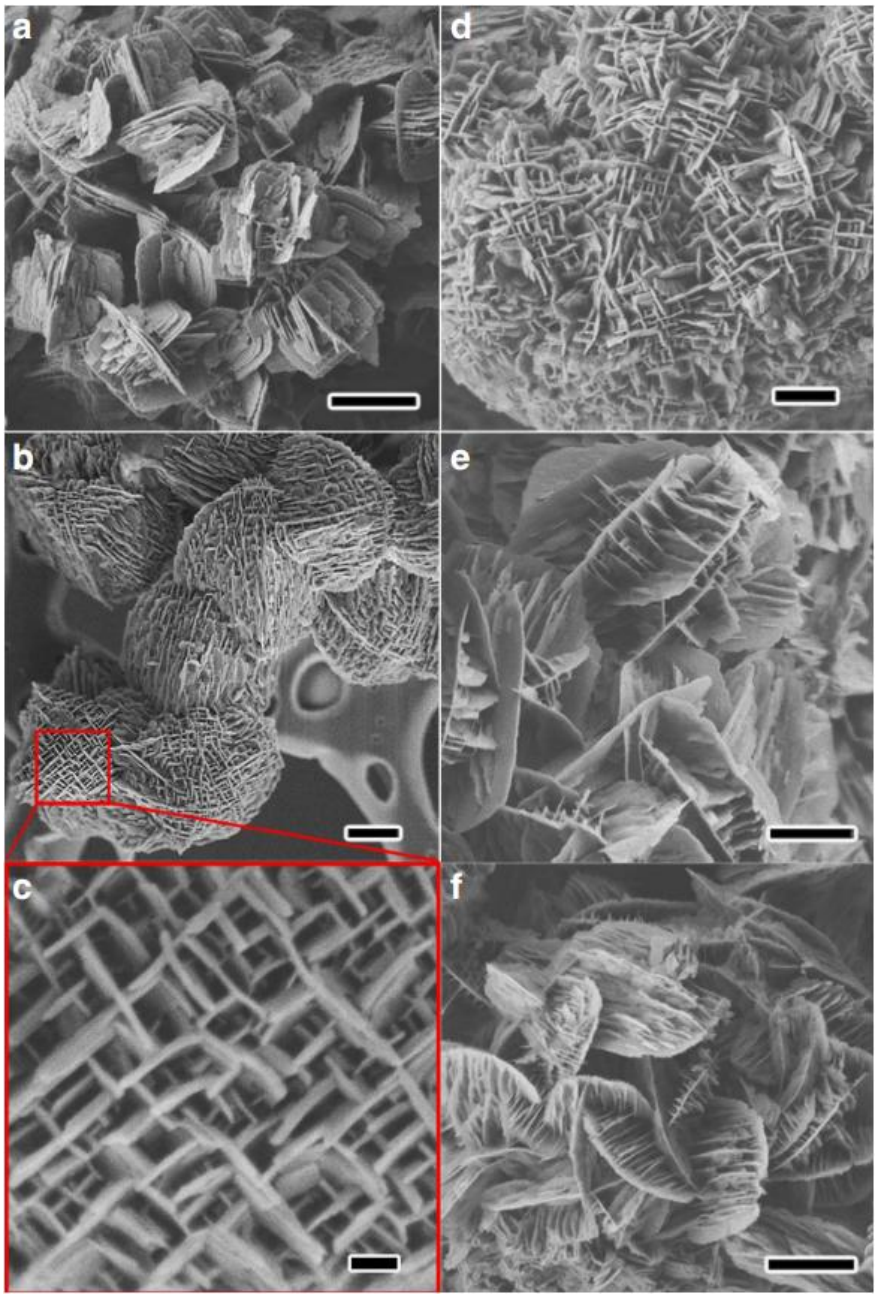

Figure 4. SEM images of as-made samples: $BC_{Ph\text{-}4\text{-}6\text{-}6}$ (**a**); $BC_{Ph\text{-}6\text{-}6\text{-}6}$ (**b**,**c**); $BC_{Ph\text{-}8\text{-}6\text{-}6}$ (**d**); $BC_{Ph\text{-}10\text{-}6\text{-}6}$ (**e**); and $BC_{Ph\text{-}12\text{-}6\text{-}6}$ (**f**), all showing the formation of single-crystalline zeolite nanosheets with 90 °C rotational boundary. The scale bars in (**a**–**f**) represent 1 mm, 500 nm, 100 nm, 500 nm, 1 mm and 1 mm, respectively [42]. Copyright Nature Publishing Group, 2014.

The nanosheet MFI zeolite with high BET surface area and mesopore volume was synthesized with $C_{22\text{-}6\text{-}6}$ and ethanol as structure-directing agents. The conversion increased by 26% with less carbon deposition in supercritical catalytic cracking of *n*-dodecane, due to high diffusion efficiency and better accessibility of acid sites resulting from the superior morphology property [44]. TPAOH was also selected as a second SDA to prepare the nanosheet MFI with different morphology and texture properties by changing its concentration [45]. The morphology of the synthesized nanosheet MFI zeolite changed from intertwined, to house-of-cards-like, and to dense packing plates with the increase of TPAOH concentration. The textural property increased firstly and then

decreased with the increase of TPAOH concentration. Tsapatsis et al. [46] successfully prepared self-pillared MFI nanosheets by repetitive branching during one-step hydrothermal crystal growth with tetra(*n*-butyl)phosphonium hydroxide solution (TBPOH) as SDA. The nanosheets (2 nm thick) resembled and formed a house-of-cards construction. The short diffusion length and high external surface area promoted the reaction of large molecules. Srivastava et al. [47] prepared the nanosheet MFI zeolite by combining two structure directing agents of tetrapropylammonium bromide (TPABr) and $C_{18\text{-}6\text{-}6}$ (Figure 5). TPABr induced the formation of microporous structure of MFI zeolite. The long hydrophobic chains of $C_{18\text{-}6\text{-}6}$ facilitated the ordered stacking of microporous zeolite layers to produce nanosheet-like morphology. Besides, it restrained the excessive growth of zeolites and induced the formation of inter-crystalline mesopores.

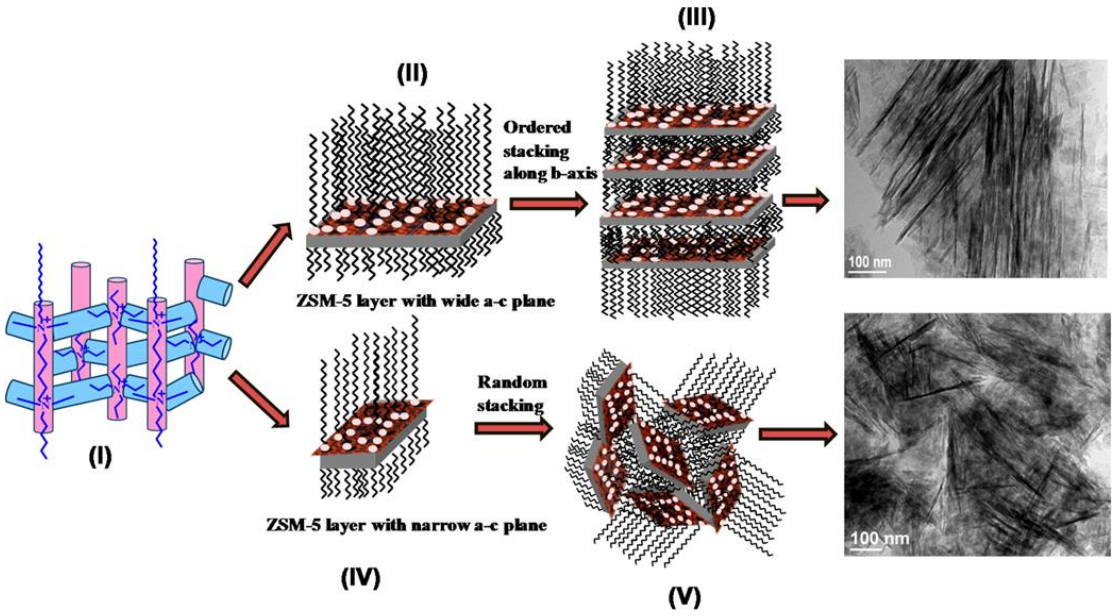

Figure 5. Proposed mechanism for the formation of ZSM-5 nanosheets in the presence of $C_{18\text{-}6\text{-}6}$ and TPABr [47]. Copyright American Chemical Society, 2016.

Besides, the nanosheet zeolite could act as an excellent supporter for loading metal nanoparticles to develop a multifunctional zeolite catalyst. It provides larger surface area to support the metal nanoparticles, thus the nanoparticles could uniformly distribute within zeolite crystals and prevent the aggregation among metal nanoparticles with the increase of loading amount. While for conventional ZSM-5 zeolite, they are only supported on the external surface, and it is easy to aggregate resulting in the decrease of BET surface area or the blockage of pore channel [48].

Overall, to synthesize the nanosheet MFI zeolite, a suitable SDA is of great necessary. The tail of SDA should be sufficiently hydrophobic to generate a bulky hydrophobic barrier in the micelle, so that the lamellar structure growth is confined around the hydrophilic tails and the nanosheet thickness can be effectively controlled. It has been proven that the hydrophobic tail (C_nH_{2n+1}) should be long enough (n = 10–22) to restrain the over growth of lamellar structure. When the hydrophobic tail is too short (n < 8), the molecules of SDA are embedded inside the micropores, resulting in a blocky zeolite [49].

The nanosheet MFI zeolite shows higher BET surface area, higher external surface area and larger mesopore volume than that of the conventional ZSM-5 zeolite, providing better textural properties for catalytic cracking reactions (Table 2). However, the duration of synthesis process is usually as long as 5 days, which is time and energy-consuming in industrial manufacture. Therefore, developing a time-saving method to prepare the nanosheet MFI zeolite is of great significant.

Table 2. Textural properties of the conventional ZSM-5 and MFI nanosheet zeolites in the references.

Sample	SDA	S_{BET} [a] ($m^2 \cdot g^{-1}$)	S_{ext} [b] ($m^2\ g^{-1}$)	V_{Tot} [c] ($cm^3\ g^{-1}$)	V_{mic} [d] ($cm^3 \cdot g^{-1}$)	V_{mes} [e] ($cm^3 \cdot g^{-1}$)	T_{thic} [f] (nm)	T [g] (d)	R [h]
ZSM-5-bulk	TPAOH	373	91	0.21	0.17	0.04	-	3	[41]
ZSM-5(6, 20, 423)	$C_{22\text{-}6\text{-}6}(Br)_2$	685	826	0.75	0.09	0.66	-	5	[41]
MFI nanosheets	$BC_{Ph\text{-}6\text{-}6\text{-}6}$	658	-	0.62	0.11	0.51	4.8	-	[42]
MFI nanosheets	$BC_{Ph\text{-}8\text{-}6\text{-}6}$	621	-	0.58	0.10	0.48	4.9	-	[42]
MFI-Al	$C_{22\text{-}6\text{-}6}(OH)_2$, C_2H_5OH	479	-	1.05	0.22	0.83	-	5	[44]
MFI-10/3	$C_{22-6-6}(Br)_2$, TPAOH	517	376	0.50	0.07	0.43	-	5	[45]
ZSM-5	$C_{18-6-6}(Br)_2$, TPABr	612	260	0.80	-	-	-	5	[47]
MFI-like	$18\text{–}N_3\text{–}18$	1190	-	1.58	-	-	1.7	-	[50]
MFI-like	18–N4–18	1060	-	1.48	-	-	2.3	-	[50]
Fe/ZSM-5-sheet	$C_{16\text{-}6\text{-}6}(Br)_2$	508	-	0.57	0.11	0.45	2–3	9	[51]
Fe/ZSM-5-sheet	$C_{16\text{-}6\text{-}6}(OH)_2$	522	-	0.65	0.12	0.53	2–3	9	[51]
MFI nanosheets	$C_{18\text{-}6\text{-}6}(Br)_2$	530	-	0.64	0.13	0.51	2.5	11	[52]
ZSM-5-S	$C_{22}\text{-}N_4\text{-}C_{22}(Br)_4$	630	439	1.18	0.15	1.03	-	5	[53]
ZSM-5-R	$C_{22}\text{-}N_4\text{-}C_{22}(Br)_4$	518	355	1.32	0.13	1.19	-	5	[53]
MesoMFI(2, OH)	$C_{22\text{-}6\text{-}6}(OH)_2$	457	393	0.85	0.08	0.77	-	12	[54]
MesoMFI(3, OH)	$C_{22\text{-}6\text{-}6\text{-}6}(OH)_3$	532	429	0.85	0.12	0.73	-	12	[54]
MesoMFI(4, OH)	$C_{22\text{-}6\text{-}6\text{-}6\text{-}6}(OH)_4$	527	535	1.15	0.10	1.05	-	12	[54]
MLMFI	$C_{biphen\text{-}8\text{-}6\text{-}6}$	519	221	0.27	0.12	0.15	3.5	5	[55]
PI-ZSM-5	$C_{22\text{-}6\text{-}6}Br_2$	698	498	0.61	0.12	0.49	-	7	[56]

[a] BET surface area; [b] External surface area; [c] Total volume; [d] Micropore volume; [e] Mesopore volume; [f] Thickness of nanosheet; [g] Times used for synthesizing the nanosheet zeolite; [h] Reference.

2.4. b-Oriented MFI Zeolite

The straight channel along *b* axis has been considered as the fast diffusion pathway due to the straight and short transport path [57]. The catalytic activity of *b*-oriented MFI zeolite was enhanced sharply when it was applied in the supercritical catalytic cracking of hydrocarbon due to ultrashort diffusion path [58]. Therefore, much attention has been attracted to prepare the MFI zeolite grown only along the *b*-axis to decrease the diffusion length. However, most of the related studies were to prepare the *b*-oriented MFI zeolite without aluminum atoms [59–61]. It is of great challenge to prepare *b*-oriented MFI zeolite containing aluminum atoms for catalytic reactions, for the difficulty on effectively controlling the growth orientation with the co-existence of silicon and aluminum atoms. Besides, it is difficult to control the *b*-orientation of MFI crystals in a bi- or multi-layer. A layer by layer method was developed to prepare the multilayer *b*-oriented ZSM-5 coatings on stainless steel slides by surface modification with TiO_2 sols for catalytic cracking of *n*-dodecane (Figure 6) [57]. The hydroxyl groups (Ti-OH) could facilitate the directional growth. Therefore, the ZSM-5 monolayer grew along the *b* axis with the guidance of TiO_2 layer during hydrothermal treatment process. Similar process was conducted several times to obtain enough mass of *b*-oriented ZSM-5 layers. The catalytic activity of *n*-dodecane cracking over *b*-oriented ZSM-5 layers increased more than 60% and the deactivation rate decreased from 17.3% to 2.3% due to the enhanced diffusion rate in *b*-oriented ZSM-5 zeolite. Overall, synthesis of *b*-oriented MFI zeolite is still in laboratory scale, and it is difficult to directly control the crystal growth.

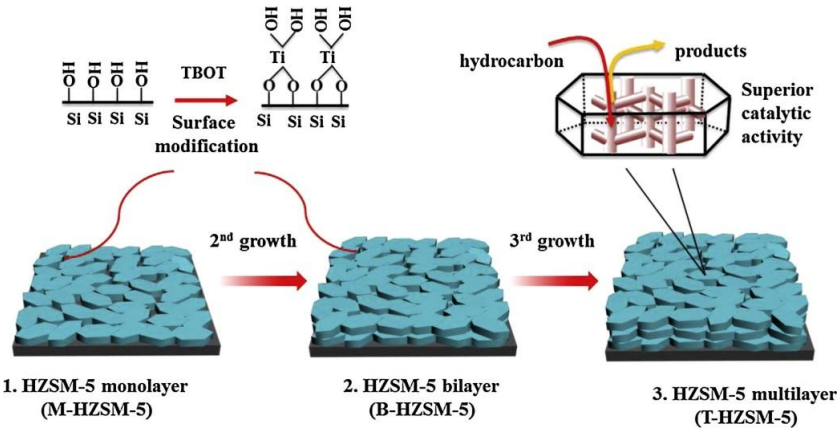

Figure 6. Scheme of the layer-by-layer hydrothermal synthesis of multilayer HZSM-5 coatings via surface modification process using titanium alkoxide solution. TBOT, tetra n-butyl ortho-titanate [57]. Copyright Elsevier, 2014.

2.5. Other Zeolite with Special Morphology

A wool-ball-like ZSM-5 (Figure 7) was prepared by a conventional hydrothermal process without adding a secondary template. It exhibited larger external surface and shorter diffusion length compared with the conventional ZSM-5 zeolite. It showed enhanced conversion rate of *n*-octane due to the improved diffusion of reactants. The conversion of isopropylbezene cracking over the wool-ball-like ZSM-5 was maintained at 80% even after reaction for 27 h, while that over conventional ZSM-5 decreased to 40% after 10 h [62]. Jalil et al. [63] prepared fibrous silica ZSM-5 zeolite (Figure 8) with the feature of high surface area (554 $m^2 \cdot g^{-1}$), a wide pore diameter (2–20 nm) and abundant strong acid sites by combining the micro-emulsion system and the zeolite crystal-seed crystallization methods. It showed high accessibility and low diffusion limitation for molecules, and excellent activity in cumene, DIPB and TIPB cracking. The cumene conversion maintained at 90% after 100 pulses, while that of the conventional ZSM-5 decreased to 50%. Hierarchical ZSM-5 fibers with macro-, meso-, and micropores were prepared by electrospinning method [64]. The macroporous structure could be regulated by controlling the rates of inner fluid during coaxial electrospinning. The synthesized hierarchical ZSM-5 hollow fibers showed higher light alkene selectivity (41.3%) and better anti-coking performance in the cracking of *iso*-butane. The conversion maintained at about 95% even after reaction for 60 h. Based on this hierarchical ZSM-5 hollow fibers, Ga_2O_3/ZSM-5 bifunctional hollow fiber catalyst was prepared and it showed enhanced catalytic activity and light alkene selectivity due to the synergistic effect of the dehydrogenation activity of Ga_2O_3 and cracking activity of ZSM-5. The highest yield of light olefins plus aromatics of *n*-butane cracking over Ga_2O_3/ZSM-5 reached to 87.6%, which was 56.3% higher than that over ZSM-5 [65]. Fu et al. [66] prepared two zeolites with different morphologies (nano-sphere and nano-rod crystallite aggregation) but with the same acid properties. The nano-sphere crystallite aggregate ZSM-5 zeolite showed better catalytic activity than that of nano-rod crystallite aggregate ZSM-5 zeolite, due to its higher diffusion efficiency and acid sites accessibility originated from its larger external surface and mesopore volume.

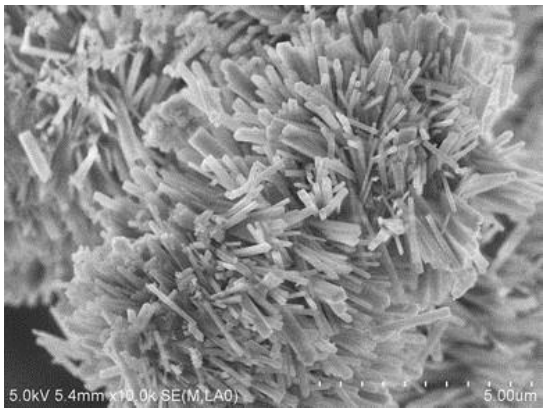

Figure 7. A wool-ball-like zeolite composed of nano-sized MFI crystals [62]. Copyright Springer, 2016.

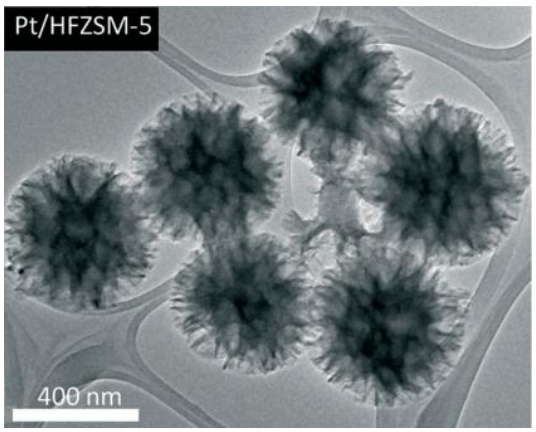

Figure 8. TEM image of fibrous ZSM-5 zeolite [63]. Copyright Royal Society of Chemistry, 2016.

3. Hierarchical ZSM-5 Zeolite

Due to the lower diffusion efficiency in micropores for the conventional ZSM-5 zeolite, much work has been done to design ZSM-5 zeolite with hierarchical porous structure to enhance the diffusion of reactants and accessibility of acid sites [14,67,68]. Garcia-Martinez et al. [19] revealed the nature of intracystalline mesopores and its connectivity by electron tomography, three-dimensional rotation electron diffraction, and high resolution gas adsorption coupled with hysteresis scanning and density functional theory. The intracystalline mesopores could act as fast channel to connect the micropores and promote the transformation of molecules, thus enhance the catalytic performance and restrain the generation of carbon deposition. It has been proven that the hierarchical ZSM-5 zeolite have a better catalytic cracking performance due to the enhanced diffusion rates and acid sites accessibility compared with conventional ZSM-5 zeolite [18,69]. Double templating with hard-template method, double templating with soft-template method, single template method and post-treatment method are all feasible for preparing the hierarchical zeolite. The textural properties of hierarchical ZSM-5 zeolite are shown in Table 3.

Table 3. Textural properties of hierarchical ZSM-5 zeolite in the references.

Sample	S_{BET} [a] ($m^2 \cdot g^{-1}$)	S_{ext} [b] ($m^2 \cdot g^{-1}$)	V_{Tot} [c] ($cm^3 \cdot g^{-1}$)	V_{mic} [d] ($cm^3 \cdot g^{-1}$)	V_{mes} [e] ($cm^3 \cdot g^{-1}$)	R [f]
MFI-PVA(3.0)	345	140	0.33	-	-	[70]
SAC-20	395	132	0.35	0.12	0.23	[71]
HZ-32-170C-2d-13	682	-	0.84	0.17	0.67	[72]
MZ5-FS-0.1-60	426	112	0.46	0.14	0.32	[73]
ZM-3	377	119	0.24	0.12	0.12	[74]
Hi-ZSM-5	433	133	0.30	0.12	0.18	[75]
HSZs-120	427	158	0.53	0.12	0.41	[76]
DS-2	391	135	0.33	0.11	0.22	[77]
HM27_AcT_AT	450	136	0.42	0.13	0.29	[78]
MFI27_6	363	-	0.38	0.08	0.3	[79]
AT 0.2-PI 0.01	487	-	0.80	0.12	0.68	[80]

[a] BET surface area; [b] External surface area; [c] Total volume; [d] Micropore volume; [e] Mesopore volume; [f] Reference.

3.1. Double Templating with Hard-Template Method

During the synthesis process of ZSM-5 zeolite, hard templates are used to be embedded within the zeolite crystals. After calcination, the hard templates were burnt out and large number of mesopores was generated. The ratio of mesopore volume to micropore volume can be adjusted by varying the number of hard templates. Viswanadham et al. [81] prepared hierarchical ZSM-5 zeolite using glucose as the second template through a steam-assisted crystallization process. Glucose was partially carbonized during the drying of synthesis gel at 170 °C in air and then acts as the hard template embedding in the zeolite crystals. The BET surface area, porosity and acidity are correlated with the concentration of glucose in the initial synthesis solution. Miyake et al. [70] selected poly vinyl alcohol (PVA) as hard template to synthesize hierarchical ZSM-5 zeolite with uniform mesopores (15 nm) by hydrothermal method. A proper amount of PVA was necessary during the synthesis process. At low content, the PVA molecules were not embedded in zeolite crystals to generate mesopores. On the contrary, large PVA would restrain the nucleation and growth of crystals.

Recently, carbon nanotubes (CNTs) were applied to prepare hierarchical ZSM-5 zeolite. The mesopores were created not via occupying the crystals by CNTs, but preserved from nucleation and initial crystallization process. Besides, the CNTs can act as inhibitors in the steam-assisted crystallization process, preventing the excessive aggregation of zeolite crystals from generating large crystals. Large inter-crystalline mesopores were generated [82]. Liu et al. [71] studied the different roles of CNTs in hierarchical ZSM-5 zeolite preparation process by hydrothermal synthesis (HTS) and steam-assisted crystallization (SAC) methods. The crystallization rate in SAC method was lower than that in HTS method after adding CNTs, resulting in a lower Si/Al ratio and higher acid amounts in the final products in SAC method. It was explained that the growth of zeolite crystals during SAC method was via reorganization of hydrogel through solid–solid transformations. The reorganization process could be enhanced by decreasing the energy barrier with the assistance of CNTs. Moreover, more mesopores were generated using SAC method than that using HTS method, which led to higher and more stable catalytic activity in *n*-decane cracking. The conversion efficiency in *n*-decane cracking was over 90% after reaction for 11.4 h, but that of the conventional ZSM-5 zeolite was 35% (Figure 9). Jiang et al. [83] firstly prepared the hydrophilic carbon to enhance the dispersion in water by sodium hypochlorite solution treatment. Then the hydrophilic carbon was used as the hard template to prepared ZSM-5 zeolite with uniformed mesopores (Figure 10). Activated carbon (AC) was also applied in the preparation hierarchical ZSM-5 zeolite by embedding within the zeolite crystals followed by combustion [84].

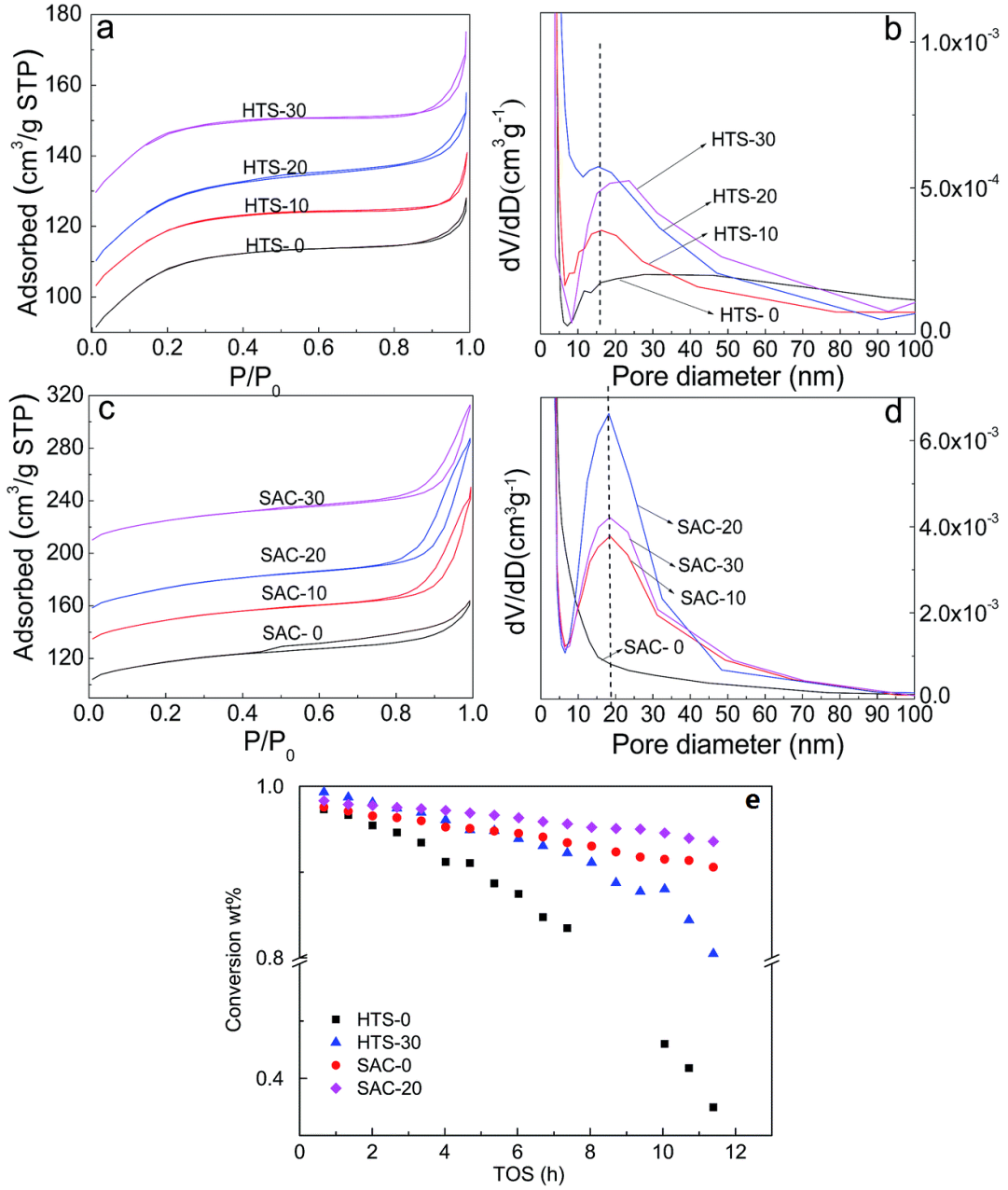

Figure 9. N_2 adsorption–desorption isothermals and pore size distribution of calcined HZSM-5: (**a**,**b**) HTS method; and (**c**,**d**) SAC method; and (**e**) conversion of *n*-decane cracking over HZSM-5 as a function of TOS. HTS-x or SAC-x, "x" denotes the percentage of mass ratio of CNTs to TEOS [71]. Copyright Royal Society of Chemistry, 2015.

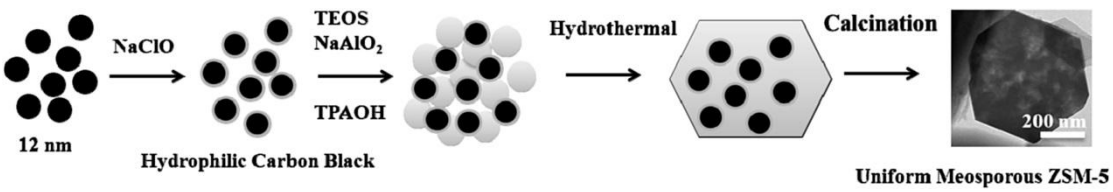

Figure 10. Synthesis scheme of mesoporous ZSM-5 using hydrophilic carbon as template [83]. Copyright Elsevier, 2016.

Although hard-template method is an effective method to prepare hierarchical ZSM-5 zeolite and adjust the texture properties by varying the number of hard templates, large number of hard templates is necessary to generate enough mesopores. Besides, much energy would cost to burn out the hard templates. Overall, the hard-template method is costly and it is still at the stage of laboratory study.

3.2. Double Templating with Soft-Template Method

Usually, another relative large organic ammonium salt is used as the second template to synthesize hierarchical ZSM-5 zeolite. By using the amphiphilic organosilanes ($[(CH_3O)_3SiC_3H_6N(CH_3)_2C_nH_{2n+1}]Cl$, TPHAC) as mesopore-directing agent, mesoporous MFI zeolite was synthesized and showed better activity especially for large molecules. The mesopore diameters can be facilely adjusted from 2 nm to 20 nm by changing the chain length of amphiphilic organosilanes [85]. Bai et al. [72] prepared scroll-like ZSM-5 zeolite with micropores, mesopores and macropores by layer-by-layer wrapping of zeolite nanosheets with the assistance of *n*-hexyltrimethylammonium bromide (HTAB). A coulombic interaction existing between HTAB and the negatively charged aluminosilicate species stabilized the zeolite nanoparticles by decreasing their surface free energy, and facilitates the formation of hierarchical ZSM-5 zeolite at short crystallization time. Wu et al. [73] prepared hierarchical ZSM-5 zeolite using cetyltrimethylammonium bromide (CTAB) and 1, 6-diaminohexane (DAH) as structure-directing agents. The mesoporous silicoalumina species generated from the aluminosilicate precursor by the inducing of CTAB firstly. Then, it was transformed to hierarchical ZSM-5 zeolite with the assistance of DAH. The encapsulated CTAB could restrain the excessive growth and dissolution of the initially formed mesoporous particles, and preserving the large mesoporosity. Hensen et al. [86] prepared hierarchical ZSM-5 zeolite by combining an amphiphilic surfactant C16MP with 1, 6-diaminohexane (DAH) as the structure-directing agents. As there was suppression reaction between two different templates during the crystal growth, it was crucial and difficult to regulate the ratio of two templates to induce the crystal growth and mesopores generation. Cationic dimethyldiallyl ammonium chloride acrylamide copolymer (PDDA) solution can also be used as soft-template to prepare hierarchical ZSM-5 zeolite. The total volume, mesopore volume and external surface area increased with the increase of PDDA content [87]. Overall, it is feasible to synthesis hierarchical ZSM-5 by double templates method if two templates play synergistic effect other than inhibiting effect. However, the cost would also increase with the addition of another SDA.

3.3. Single Templating Method

To avoid the suppression reaction between two different templates during the crystal growth and decrease the preparation cost, many studies have been conducted to prepare hierarchical ZSM-5 zeolite with single template. Wu et al. [74] prepared mesoporous ZSM-5 microspheres using *n*-hexylamine as the template. With the direction induction of *n*-hexylamine, small crystals generated and assembled to uniform cauliflower-like microspheres successively. Besides, the average diameter of the mesoporous zeolite could be effectively regulated by adjusting the alkalinity of the preparation solution. The mesoporous ZSM-5 zeolites with improved diffusion efficiency and acids accessibility showed better performance than the conventional ZSM-5 zeolite. TPAOH, a conventional microporous template, can be used as the single SDA to prepare hierarchical ZSM-5 zeolite [75,76]. Hua et al. [76] successfully prepared the hierarchical ZSM-5 zeolite using only TPAOH as the SDA through one-step hydrothermal process at a relatively low temperature of 100 °C, and they proposed a "nucleation/growth-demetallation/recrystallization" mechanism during the hydrothermal synthesis process. Initially, the precursor species nucleated and grew under the protection of aluminum complexes and TPA^+ cations. Then basic etching became obvious with the consumption of aluminum complexes and TPA^+ cations, resulting in the mesoporous structure. Finally, the dissolved species recrystallized and grew on the external surface of the zeolite crystals (Figure 11). During the catalytic cracking of 1, 3, 5-triisopropylbenzene (TIPB), the hierarchical ZSM-5 zeolite showed conversion rate

of 80% with little carbon deposition, while that of the conventional ZSM-5 was only 55% with much more carbon deposition.

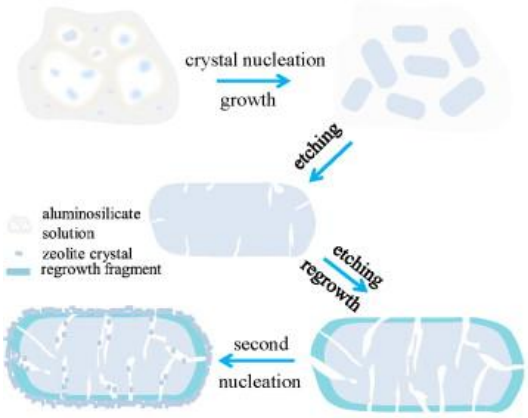

Figure 11. The mechanism for the formation of HSZs [76]. Copyright Elsevier, 2015.

3.4. Post-Treatment Method

3.4.1. Alkaline Etching

Among the alkaline etching methods, sodium hydroxide (NaOH) etching method is the most widely used to prepare the hierarchical zeolite. The silicon is selectively dissolved by NaOH treatment to generate substantial mesoporosity. The catalytic performance and catalytic lifetime can be effectively enhanced by this post-treatment method [77–79,88,89]. After alkali treatment, although more carbon deposited on ZSM-5 zeolite in *n*-hexane cracking, it showed smaller deactivation rate due to the increased external surface area, mesopore volume and pore mouth, which made ZSM-5 zeolite less sensitive to carbon deposition [90]. A proper Si/Al ratio of 25–50, however, is necessary to obtain the hierarchical zeolite with excellent texture properties. High aluminum content could stabilize the surrounding silicon atoms preventing their dissolution, which leads to few mesopores, while, for low aluminum content, large number of the zeolites could be dissolved resulting in low productivity and large pores [91]. Yuan et al. [92] developed a new method to prepare the hierarchical ZSM-5 zeolite by post-treatment with different concentration of sodium aluminum solution ($NaAlO_2$). It is a more moderate alkaline etching method compared with NaOH etching method. It extracted Si species selectively and protected the structure by repairing the defects resulting from desilicication with Al species at the same time. Wu et al. [80] synthesized the mesoporous ZSM-5 zeolite by desilication in combined basic solution of NaOH and piperidine. The addition of piperidine prevented the excessive dissolution of Si species by NaOH, resulting in the controlled desilication within the crystals and maintained the micropores simultaneously. The newly formed mesopores enhanced the accessibility of acid sites in the micropores and shortened the diffusion path length, resulting in a higher catalytic performance and a longer lifetime in hydrocarbon cracking. However, after treatment with inorganic hydroxides, ZSM-5 zeolite was transformed to Na-ZSM-5. Additional ion exchange with NH_4NO_3 solution was necessary to obtain H-ZSM-5 zeolite. This disadvantage could be neglected with organic hydroxides instead of inorganic hydroxides. As the organic hydroxide is less active over Si dissolution than inorganic hydroxides, the dissolution of Si species is more controllable and more Al is dissolved. The Si/Al ratio decreased less in organic hydroxide solution than that in inorganic hydroxide solution, resulting in negligible change of acid property after organic hydroxide treatment (Figure 12) [93]. A meso-ZSM-5 zeolite was prepared by post-treatment of ZSM-5 zeolite with tetramethylammonium hydroxide (TMAOH) or tetraethylammonium hydroxide (TEAOH) [26]. The catalytic cracking activity of the hierarchical ZSM-5 zeolites increased significantly compared with parent ZSM-5 zeolite.

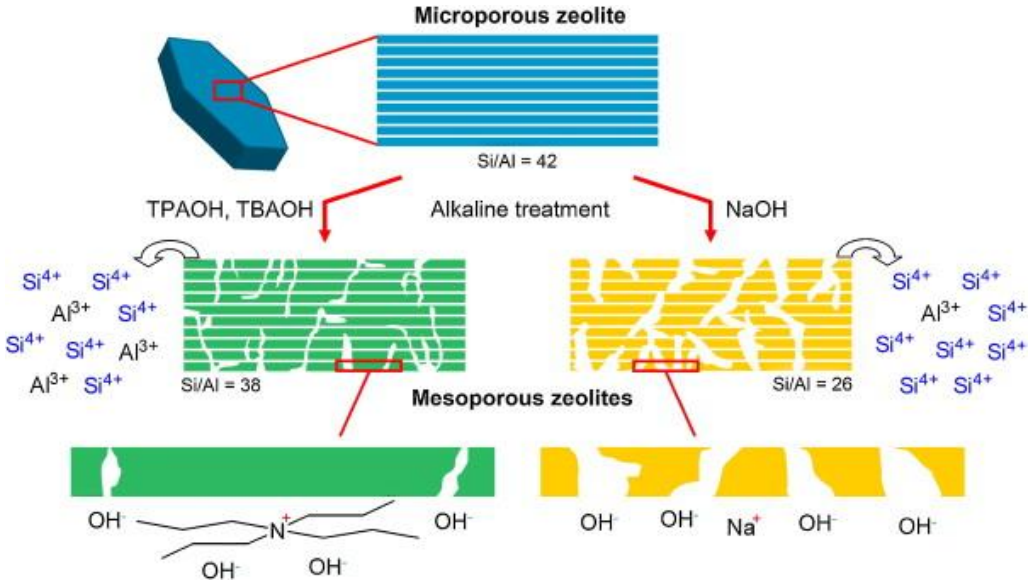

Figure 12. Pictorial comparison of zeolite desilication by tetraalkylammonium hydroxides and sodium hydroxide [93]. Copyright Elsevier, 2009.

3.4.2. Fluoride Etching

Post-treatment of ZSM-5 zeolite with hydrofluoric acid (HF) solution is also an effective approach to prepare the hierarchical zeolite. The crystallinity of the treated ZSM-5 zeolites does not change observably. The Al species is selectively dissolved resulting in the increase of external surface area and mesopore volume, and decrease of acid sites with a higher Si/Al ratio. The catalytic activity was enhanced with the additional mesoporous after HF treatment [94]. While in NH_4F-HF mixed aqueous solutions, large bifluoride ions (HF_2^-) generated due to chemical equilibrium, which was at least four to five times faster than HF in Si dissolution, as well as Al extraction simultaneously. As a result, the Si/Al ratio and acid sites were similar to the parent ZSM-5 zeolite, and large mesopores and macropores were generated without destroying the intrinsic micropores. The interfaces between intergrown crystals which act as diffusion barriers were preferentially dissolved during NH_4F-HF treatment, resulting in a higher crystalline domains (Figure 13) [95,96]. Besides, the silanols in treated samples were less than that in the parent ZSM-5 zeolite, which restrained the generation of carbon deposition on these sites [95]. As the acid property was similar with the parent ZSM-5 zeolite, the remarkably increased catalytic activity could be attributed to the high diffusion rate originated from the additional mesopores and macropores [97]. Overall, fluoride etching is an effective and fast approach to prepare hierarchical zeolite. However, HF is dangerous for human and it is troublesome when it is applied in industrial manufacture.

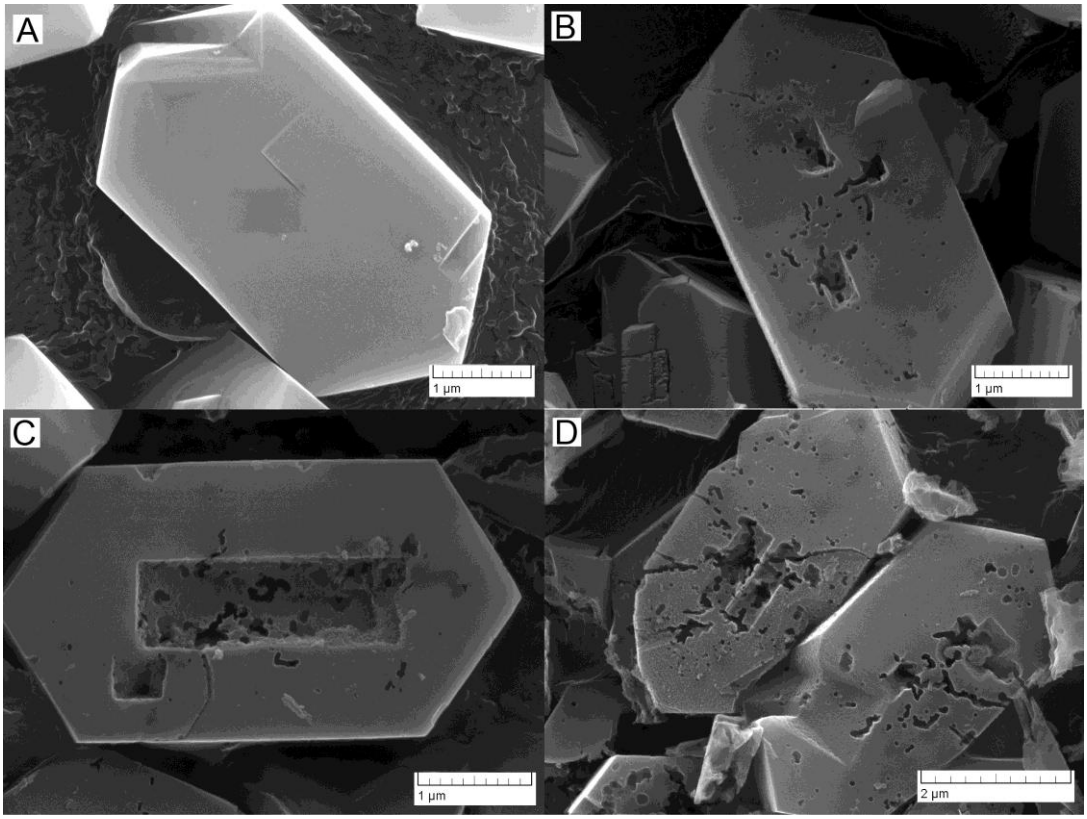

Figure 13. SEM images of ZSM-5 crystals treated by NH_4F-HF solutions at 293 K. The NH_4F-HF solutions contain different amounts of HF (0.05, 0.1, and 0.5 mol·L^{-1}) and a constant amount of NH_4F (2.5 g per 15 mL solution): (**A**) treated by a 0.05 mol·L^{-1} solution for 30 s; (**B**) treated by a 0.1 mol·L^{-1} solution for 30 s; (**C**) treated by a 0.5 mol·L^{-1} solution for 10 s; and (**D**) treated by a 0.5 mol·L^{-1} solution for 30 s [95]. Copyright American Chemical Society, 2013.

4. Nano-Sized ZSM-5 Zeolite

Although addition of mesopores to conventional ZSM-5 zeolite is an effective way to enhance the catalytic activity of ZSM-5 zeolite, the most efficient method is to prepare nano-sized ZSM-5 zeolites, which can dramatically increase the number of pore mouths and increase the accessibility of acid sites in the micropores. As nano-sized ZSM-5 zeolites with shorter diffusion length favored the adsorption and desorption of reactants in the micropores compared with the micro-sized zeolite, the catalytic cracking activity increased with the decrease of crystal size [15,98–100]. Tago et al. [101] studied the catalytic performance of ZSM-5 zeolite with macro-size (2300 nm) and nano-size (90 nm) in naphthene cracking. For macro-sized ZSM-5, the carbon deposition formed at the beginning of the reaction resulting in quick deactivation. While for nano-sized ZSM-5 zeolite, it showed higher light alkene selectivity, more stable activity and less carbon deposition. They also studied the effect of crystal size of ZSM-5 zeolite on the rate-limiting step of the *n*-hexane cracking using the Thiele modulus, and they concluded that the cracking reaction could be proceed when the crystal size was in nano-scale [102]. Besides, ZSM-5 zeolite with short diffusion length facilitated the transport of BTEX (carbon precursors), thus preventing the formation of carbon deposition, which improved the catalytic stability [99,100,103,104]. The nano-sized ZSM-5 zeolite can be synthesized by hydrothermal method or bead milling method. The textural properties of nano-sized ZSM-5 zeolite in the references are shown in Table 4.

Table 4. Textural properties of nano-sized ZSM-5 zeolite in the references.

Sample	P [a]	S_{BET} [b] ($m^2 \cdot g^{-1}$)	S_{ext} [c] ($m^2 \cdot g^{-1}$)	V_{Tot} [d] ($cm^3 \cdot g^{-1}$)	V_{mic} [e] ($cm^3 \cdot g^{-1}$)	V_{mes} [f] ($cm^3 \cdot g^{-1}$)	R [g]
H_2O/Si = 30	253	400	40	0.28	0.17	0.11	[98]
H_2O/Si = 8.3	106	403	49	0.56	0.17	0.39	[98]
H-MFI(1)	40–45	-	-	0.30	0.12	0.18	[99]
Z-0.02C-0.08S	20–50	416	271	0.30	0.07	0.13	[105]
B-2	-	424	42	0.21	0.13	0.08	[106]
ZNA-373	20–40	536	403	0.89	0.05	0.84	[107]
Z60-AT	30–500	430	79	-	-	-	[108]

[a] Particle size; [b] BET surface area; [c] External surface area; [d] Total volume; [e] Micropore volume; [f] Mesopore volume; [g] Reference.

4.1. Synthesis of Nano-Sized ZSM-5 Zeolite by Hydrothermal Method

Hydrothermal method is the most widely used process to prepare nano-sized ZSM-5 zeolite. The amount of water, pre-aging time and pre-aging temperature are closely related to the crystal size. Usually, the zeolite crystal size decreases with the increase of pre-aging time and pre-aging temperature, which could facilitate nucleation of nanocrystals in the pre-aging stage. The nano-sized ZSM-5 zeolites showed a better catalytic activity, a longer lifetime and less carbon deposition compared with large-sized ZSM-5 zeolite during *n*-hexane cracking [98]. ZSM-5 zeolite with uniform size of 30 nm was prepared by pre-aging at low temperature (80 °C) and then high temperature hydrothermal treatment (175 °C) [109]. The concentration of initial synthesis gel facilitated the generation of nucleation centers. At pre-aging stage, the number of critical sized nuclei increased. Finally, the high temperature promoted the complete growth of crystals. Wang et al. [105] developed a facile route to prepare nano-sized ZSM-5 zeolite using silicate-1 as seeds with the assistance of CTAB. The seeds induced the aluminosilicates into ZSM-5 phase on their surface. While CTAB could restrain the intergrowth and secondary growth of crystal nucleus, thus large number of nanocrystals formed and assembled into zeolite aggregates. The prepared ZSM-5 zeolites showed a uniform morphology with 400–600 nm, aggregation with 20–50 nm crystals, a large external surface area (273 $m^2 \cdot g^{-1}$) and large mesopore volume (0.31 $cm^3 \cdot g^{-1}$) (Figure 14). Besides, if there is no metal cation in the synthesis gel, the proton formed ZSM-5 zeolite can be directly obtained simply by calcining the products after hydrothermal treatment without ion exchange with NH_4NO_3 [87]. It was a time-saving and energy-saving procedure.

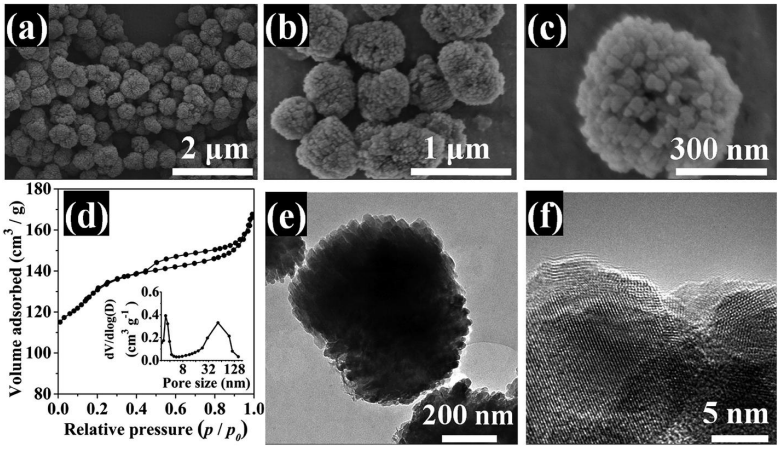

Figure 14. The morphology and textural property of N-ZSM-5: (**a**–**c**) SEM images under different magnification; (**d**) N_2 adsorption/desorption isotherm and BJH pore size distribution; (**e**) low magnification TEM image; and (**f**) high magnification TEM image [105]. Copyright Royal Society of Chemistry, 2016.

Zeolite synthesized using SDA is uneconomical and environmental unfriendly due to vast exhaust gas generated by calcination, thus it is significant to prepare nano-sized ZSM-5 zeolite without using SDA. Larsen et al. [110] successfully synthesized nano-sized ZSM-5 zeolite with the assistance of seeds by regulating the synthesis parameters. A basic solution with pH between 9 and 11.5 was necessary to facilitate the nucleation of crystals. A proper amount of seeds (0.35 wt %) provides enough nucleation and growth sites. The optimum temperature and time is 165 °C and 14–24 h to promote the complete growth of crystals. Nano-sized ZSM-5 zeolite prepared with seed-assisted method showed uniform crystal size (70–150 nm), high crystallinity and high hydrothermal stability. They showed a better activity and higher light alkene selectivity than the conventional ZSM-5 zeolite in catalytic cracking of naphtha (Figure 15) [106].

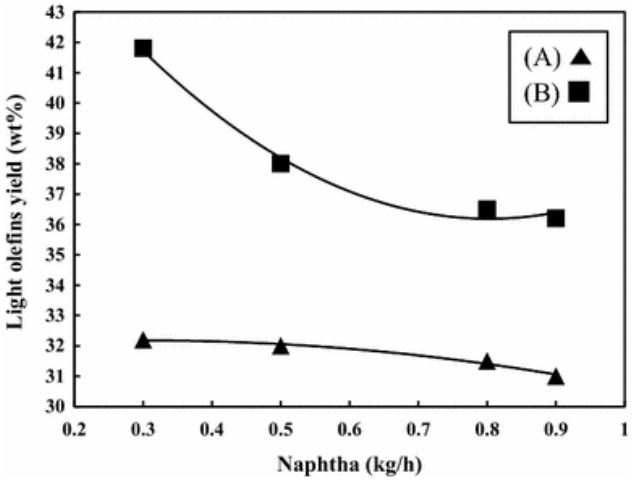

Figure 15. Light olefins yield depending on the naphtha feed rate in fluidized catalytic cracking over steamed micro-spherical catalyst prepared with: (**A**) commercial ZSM-5 (filled triangle); and (**B**) ZSM-5 synthesized with crystalline seed (filled square) (reaction condition: naphtha/steam ratio (*wt*/*wt*) = 4, contact time = 2 s, catalyst/oil = 50, reactor temperature = 680 °C, regeneration temperature = 720 °C) [106]. Copyright Springer, 2016.

However, it is difficult to separate nano zeolite from the synthesis gel due to the small crystal size, which limits its application in practical application. Aiming at overcoming this disadvantage, monolithic ZSM-5 nanoparticle aggregates were prepared by converting Al-SBA-15 to ZSM-5 zeolite. Large nanoparticles aggregated and formed a big monolithic ZSM-5 zeolite, which was easy to be separated from the solution. Besides, this monolithic ZSM-5 nanoparticle aggregate contained large mesopore volume (Figure 16). The crystallinity and inter-crystal mesoporosity could be regulated by adjusting the parameters during the synthesis process. The crystallinity and crystal size increased with the increase of hydrothermal temperature. Proper hydrothermal temperature and time were necessary to promote the nucleation and growth of crystals and prevent the over growth simultaneously. At a proper SDA content (TPA^+/Si = 1.5), the pore volume of the final obtained zeolite reached to 0.58 $cm^3 \cdot g^{-1}$, which was attributed to the enhancement of crystal nucleation by SDA. While at a high content (TPA^+/Si = 3.5), the pore volume decreased to 0.21 $cm^3 \cdot g^{-1}$, due to the highly compacted nanoparticles under high content of SDA [107].

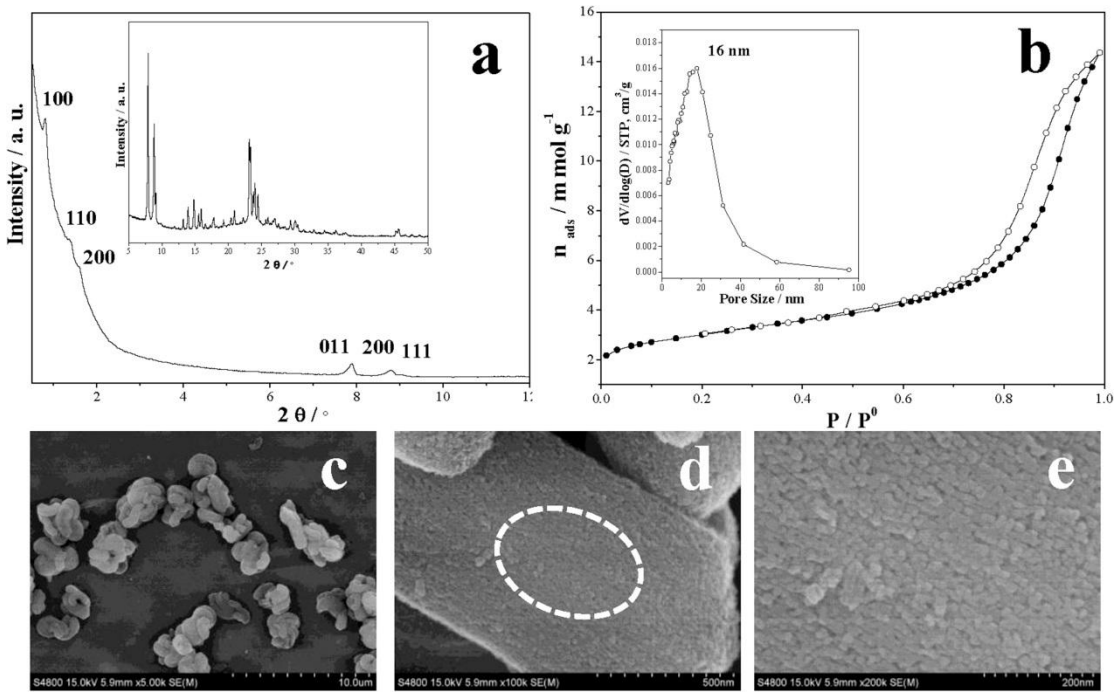

Figure 16. XRD, N_2-adsorption, and SEM results for ordered mesoporous ZSM-5 nanoparticle aggregates (ZNA) by controlling the arrangement of nanoparticles. (**a**), XRD pattern; (**b**), N_2 adsorption-desorption; (**c**–**e**), SEM images [107]. Copyright Elsevier, 2016.

4.2. Synthesis of Nano-Sized ZSM-5 Zeolite by Bead Milling Method

Inagaki et al. [108,111] creatively developed a new method to prepare nano-sized ZSM-5 zeolite by bead milling of the micro-sized ZSM-5 zeolite. After bead milling under high agitation speed of 3000 rpm, the large zeolite crystals were broken into nano-sized zeolites. The nano-sized zeolites showed higher light alkene selectivity than the conventional ZSM-5 zeolite in *n*-hexane cracking at 650 °C. However, the outer zeolite framework was destroyed, resulting in pore blockage, sharp decrease of BET surface area and crystallinity. Then, the damaged part could be removed by alkali treatment or recovered by recrystallized on the external surface of the nanoparticles, resulting in a high crystalline zeolite. The desired ZSM-5 nanoparticles showed a high and stable catalytic cracking activity (Figure 17). Besides, it was significant that the nano-sized ZSM-5 zeolite could be produced in a large scale to satisfy the actual requirement in practical industrial manufacture.

Overall, the crystal size of ZSM-5 zeolite can be controlled by regulating the parameters during the hydrothermal process only in laboratory scale. It was difficult to separate the nanoparticles from the synthesis solution due to their intrinsic colloidal property. It would applicable to prepare nanoparticle aggregation to avoid the separation problem. Besides, the stability of nano-sized zeolite at high temperature is lower than that of the micro-sized zeolite, which limits its application in industrial manufacture.

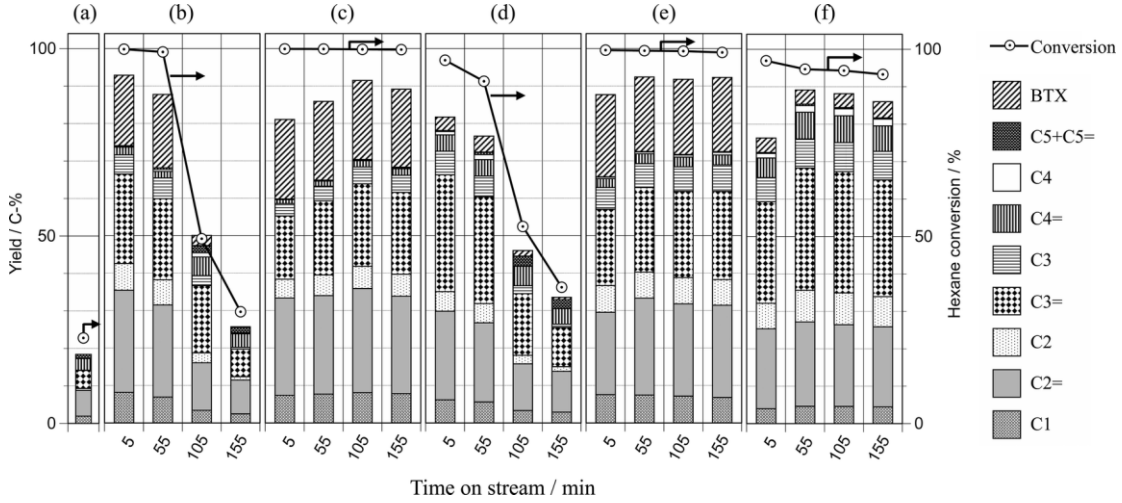

Figure 17. The conversion of hexane and product yields in hexane cracking at 650 °C over various ZSM-5 catalysts: (**a**) no catalyst; (**b**) parent ZSM-5; (**c**) acid-treated ZSM-5 micron; (**d**) milled ZSM-5; (**e**) milled and recrystallized ZSM-5; and (**f**) milled, recrystallized and acid-treated ZSM-5 [111]. Copyright Royal Society of Chemistry, 2015.

5. Adjustment of Acid Properties

For catalytic cracking of hydrocarbons, acid catalysis is dominant. Acid properties of ZSM-5 zeolite, including acid amount, acid strength and acid types, are significant for hydrocarbon cracking. All of these parameters show direct influence on the catalytic activity, product selectivity and carbon deposition during hydrocarbon cracking.

5.1. Acidity Strength

Both weak acid sites and strong acid sits exist in ZSM-5 zeolite. They play different role in hydrocarbon cracking. It has been proven that during the catalytic cracking of 1-pentene, the reaction pathway can be dominated by the acid strength of catalyst by influencing the activation energy of reaction. The weak acid sites prefer to crack 1-pentene to propylene. The strong acid sites prefer to crack 1-pentene to ethylene. Then, the ratio of propylene to ethylene can be controlled between 1.2 and 7.9 by adjusting the acid strength of ZSM-5 zeolite [112].

Besides, the acid strength of ZSM-5 zeolite can be modified by synthesizing isomorphous ZSM-5 zeolites. They are prepared by replacing the aluminum (Al) source with gallium (Ga) source or iron (Fe) source in the synthesis solution. The acid strength of isomorphous ZSM-5 zeolites increased as the following order: MFI-Fe < MFI-Ga < MFI-Al. Due to the decrease of the acidity strength, the cracking products are easier to desorb, which may restrain the second reaction between light alkenes generate from the primary cracking reaction, resulting in higher light alkene selectivity (Figure 18) and less carbon deposition [44]. Hodoshima et al. [113] prepared ZSM-5 zeolite containing Fe, Ga and Al simultaneously. The acid strength of Fe-Ga-Al ZSM-5 zeolite is weaker than that of the conventional ZSM-5 zeolite, which enhanced the selectivity of propylene and suppressed the generation of carbon deposition. However, for ZSM-5 zeolite containing Fe, the acid strength was too weak and the activation energy was not enough to catalytic cracking hydrocarbon effectively [114].

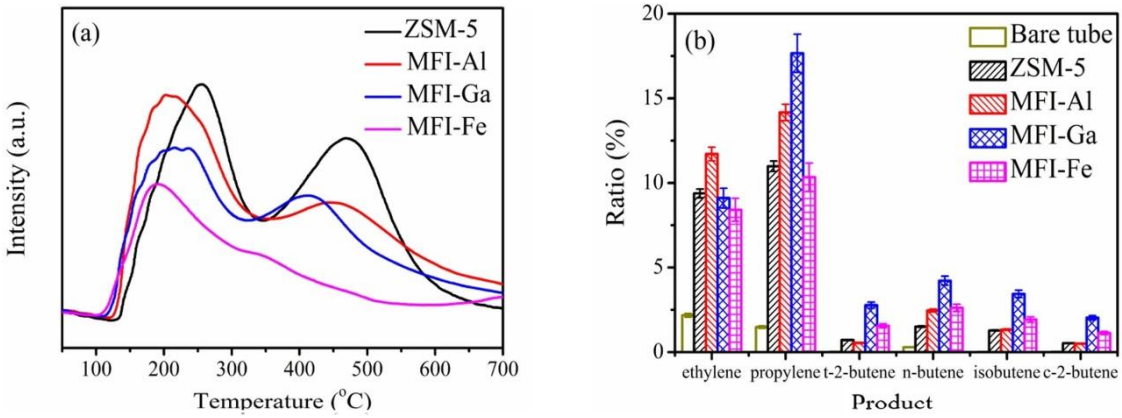

Figure 18. NH_3-TPD profiles of the isomorphous MFI nanosheet zeolites (**a**) and light alkenes selectivity (**b**) of *n*-dodecane cracking at 550 °C under 4 MPa [44]. Copyright Elsevier, 2017.

5.2. Acid Amount

ZSM-5 zeolite with excess acid amount will result in the overreaction of reactants and generating much carbon deposition. Therefore, the catalytic activity decreases quickly due to the coverage of acid sites and blockage of pore channels by carbon deposition.

One method to change the acid amount is to prepare zeolite with different Si/Al ratio. The acid amount decreases with the increase of Si/Al ratio. ZSM-5 zeolite with low Si/Al ratio would facilitate the catalytic conversion but promote the generation of carbon deposition simultaneously, leading to quick deactivation due to the coverage of acid sites and pore blockage by carbon deposition. A stable catalytic activity with less carbon deposition can be obtained by increasing the Si/Al ratio moderately. While increasing Si/Al ratio further, the catalytic activity decreased due to decrease of acid sites [115].

The other approach is to modify ZSM-5 zeolite with element or compound. ZSM-5 zeolite after gold modification showed a reasonable number of strong acid sites, resulting in higher light alkene selectivity during catalytic cracking of light diesel [116]. During the catalytic cracking of hydrocarbon, ZSM-5 zeolite with less strong acid site showed higher light alkene selectivity but lower conversion rate, because decreasing strong acid sites would restrain the secondary reaction between the primary products [117]. Phosphorus modification of ZSM-5 zeolite is an effective method to enhance its catalytic cracking performance. The acid amount decreases with the increase of phosphorus content, especially for strong acid amount. When the acid sites decrease to some extent after phosphorus modification, it could avoid the overreaction of reactants on acid sites and generation of carbon deposition, resulting in a stable catalytic activity with high light alkene selectivity in supercritical catalytic cracking of *n*-dodecane (Figure 19). The gas generation rate reached to 68% at the phosphorus content of 0.5 wt %, which was 21% higher than that of the parent ZSM-5 zeolite [118]. Furthermore, it has been found that co-modification of ZSM-5 zeolite with phosphorus and metal cation is effective method to enhance the catalytic activity and stability. Mg, Ca, La, and Zr were introduced into the phosphorus-modified ZSM-5 zeolites, respectively and they showed better catalytic activity with less carbon deposition compared with the parent ZSM-5 zeolite [119]. The acidity of lanthanum and phosphorus co-modified ZSM-5 zeolite decreased with the increase of lanthanum content, while the basicity increased with increasing lanthanum content [120,121]. The basicity could restrain the hydrogen transfer activity and enhance the generation of light alkene. Therefore, ZSM-5 zeolites with moderate acidity and basicity after lanthanum modification showed better catalytic activity and higher light alkene selectivity. Similarly, nickel and iron were introduced into phosphorus-modified ZSM-5 zeolite by impregnating method. They interacted with pre-introduced phosphorus, resulting in the recovery of partial Brønsted acid sites which were neutralized by phosphorus modification. The increased Brønsted acid sites enhanced the cracking of hydrocarbon and selectivity of light alkenes [122,123].

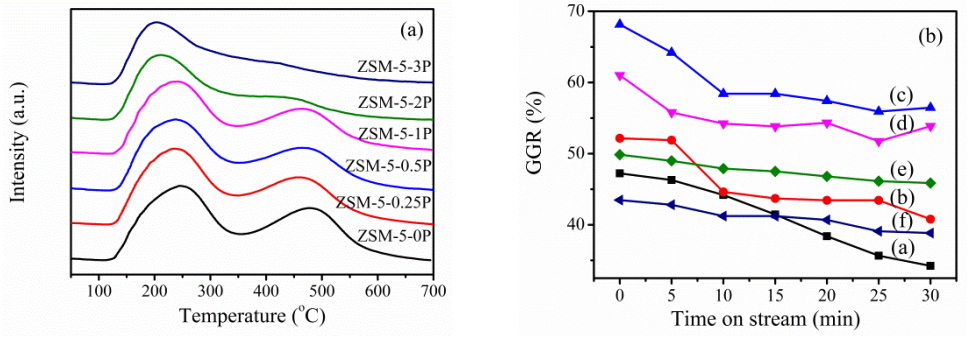

Figure 19. NH_3-TPD profiles (**a**); and GGR variation of *n*-dodecane cracking (**b**) over phosphorus-modified ZSM-5 zeolites for 30 min at 550 °C under the pressure of 4 MPa: (**a**) ZSM-5-0 P; (**b**) ZSM-5-0.25 P; (**c**) ZSM-5-0.5 P; (**d**) ZSM-5-1 P; (**e**) ZSM-5-2 P; and (**f**) ZSM-5-3 P [118]. Copyright Elsevier, 2017.

5.3. Surface Acid Sites

Too many acid sites on the external surface of ZSM-5 zeolite could lead to large carbon deposition on the external surface during the catalytic reactions, which would cover the surface or block the pore mouth. Then, the acid sites in the micropores cannot catalyze the reactants effectively, resulting in quick deactivation. Thus, the catalytic activity can be enhanced by passivating the acid sites on the external surface.

A post-synthetic HNO_3 treatment method was developed to selectively remove the acid sites on the external surface [124]. As a result, the treated ZSM-5 zeolite maintained high catalytic activity (about 96%) with little carbon deposition (49.7 $mg \cdot g^{-1}$) even after reaction for 455 min, while, for the parent ZSM-5 zeolite, the conversion decreased to about 67% with large carbon deposition (120 $mg \cdot g^{-1}$) (Figure 20). However, this method is only effective to treat zeolite prepared in the absence of organic structure-directing agent (OSDA). For zeolite prepared with the assistance of OSDA, not only the external surface Al but also large framework Al would be dissolved by HNO_3 treatment.

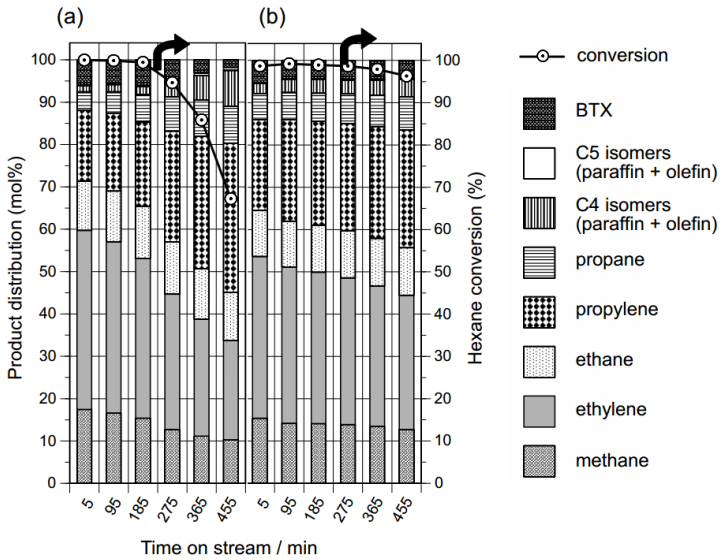

Figure 20. Hexane conversion and product yield (mol %) for hexane cracking over zeolite catalysts at 650 °C. The catalysts are: (**a**) parent H^+-ZSM-5 OSDAF (Si/Al = 16.4); and (**b**) deAl(6.0)-ZSM-5 (Si/Al = 22.6). W/F = 19.8 g-cat. h mol^{-1}, and partial pressure of hexane = 5 kPa. BTX means the mixture of benzene, toluene and xylenes [124]. Copyright American Chemical Society, 2013.

Rimer et al. [38] designed ZSM-5 zeolite with passivated surface acidity by adding silicalite-1 shell on the external surface. Few acid sites exist on the external surface of ZSM-5 zeolite after adding silicalite-1 shell. Consequently, the carbon deposition on the external surface can be suppressed, resulting in high product selectivity.

The external acid sites were deactivated by deposition of MgO on the external surface of ZSM-5 zeolite [125]. Magnesium acetate is selected as the precursor, which polymerizes to large-molecule coordination compounds in aqueous solution and cannot enter into the micropores. Then, MgO is deposited on the external surface after calcination and deactivated the external acid sites. The amount of carbon deposition decreased after MgO modification.

Besides, a mechanochemical approach using powder composer was used to deactivate the surface acid sites. Shear force was imposed on the surface and selectively deactivated the acid sites on external surface. After mechanochemical treatment, ZSM-5 zeolite exhibited little activity on TIPB cracking, indicating few acid sites existed on the external surface of ZSM-5 zeolite [126].

6. Conclusions and Outlook

Many studies have been done to enhance the catalytic cracking performance of ZSM-5 zeolite including catalytic cracking activity, selectivity of light alkenes and carbon deposition in recent years. In this review, factors affecting the catalytic performance of ZSM-5 zeolite in hydrocarbon catalytic cracking were discussed from the aspects of ZSM-5 zeolite with special morphology, hierarchical ZSM-5 zeolite, nano-sized ZSM-5 zeolite and acid properties. They are all effective ways to enhance the catalytic cracking performance of ZSM-5 zeolite. The diffusion length decrease and diffusion efficiency of molecule can be enhanced by preparing ZSM-5 zeolite with special morphology. Hierarchical ZSM-5 zeolite can be obtained by template-assisted method or post-treatment method. The accessibility of acid sites in the micropores is improved by the additional mesopores or macropores. Especially for post-treatment method, it is convenient to obtain ZSM-5 zeolite with hierarchical pore structure. Nano-sized ZSM-5 zeolites with short diffusion length favor the cracking of hydrocarbon. Acid property is crucial for catalytic cracking reactions. By adjusting the acid properties, the catalytic activity and light alkene selectivity can be improved efficiently and the formation of carbon deposition can be suppressed.

Each method has its own advantage and disadvantage, it would be better to integrate the advantages of each method and develop ZSM-5 zeolite with superior activity. By modifying nano-sized ZSM-5 zeolite with elements or compounds, ZSM-5 zeolite has the feature of short diffusion pathway and moderate acid property simultaneously, which would result in high catalytic conversion rate, high light alkene selectivity and less carbon deposition during hydrocarbon cracking. Preparing nano-sized ZSM-5 zeolite with hierarchical pore structure could decrease the diffusion length as well as increase the accessibility of acid sites in the micropores. Moreover, developing bifunctional catalysts by modification of MFI nanosheet zeolite with another catalyst is feasible to enhance the catalytic performance of ZSM-5 zeolite.

Above all, most of these strategies to enhance the catalytic cracking performance are still in laboratory scale. Overall, elimination of compounds potentially harmful for the environment such as the hard/soft templates and zeolite structure-directing agent (SDA) remains a great challenge. It is difficult to separate the nano-sized ZSM-5 zeolite in large scale and it is costly to synthesize nanosheet zeolite hydrothermally with long time. Few studies have been reported to offer the possibility to scale-up in a cost-effective way. Therefore, developing a cheap and effective way to prepare ZSM-5 zeolite with excellent activity is significate for manufacture application.

Finally, the above approaches are not only effective for catalytic cracking of hydrocarbon, but also suitable for other catalytic reactions. By synthesis of ZSM-5 zeolite with special morphology, hierarchical zeolite and nano-sized zeolite, the diffusion efficiency, diffusion length and accessibility of acid sites can be enhanced and facilitate the catalytic reaction efficiency.

Acknowledgments: This review was sponsored by the National Natural Science Foundation of China (Grant No. 21306147).

Conflicts of Interest: The authors declare no conflict of interest.

References

1. Emori, E.Y.; Hirashima, F.H.; Zandonai, C.H.; Ortiz-Bravo, C.A.; Fernandes-Machado, N.R.C.; Olsen-Scaliante, M.H.N. Catalytic cracking of soybean oil using ZSM5 zeolite. *Catal. Today* **2017**, *279*, 168–176. [CrossRef]
2. Zhang, Q.; Liu, G.; Wang, L.; Zhang, X.; Li, G. Controllable Decomposition of Methanol for Active Fuel Cooling Technology. *Energey Fuels* **2014**, *28*, 4431–4439. [CrossRef]
3. Li, W.; Li, G.; Jin, C.; Liu, X.; Wang, J. One-step synthesis of nanorod-aggregated functional hierarchical iron-containing MFI zeolite microspheres. *J. Mater. Chem. A* **2015**, *3*, 14786–14793. [CrossRef]
4. Aziz, A.; Kim, K.S. Investigation of tertiary butyl alcohol as template for the synthesis of ZSM-5 zeolite. *J. Porous Mater.* **2015**, *22*, 1401–1406. [CrossRef]
5. Xu, D.; Swindlehurst, G.R.; Wu, H.; Olson, D.H.; Zhang, X.; Tsapatsis, M. On the Synthesis and Adsorption Properties of Single-Unit-Cell Hierarchical Zeolites Made by Rotational Intergrowths. *Adv. Funct. Mater.* **2014**, *24*, 201–208. [CrossRef]
6. Cundy, C.S.; Cox, P.A. The hydrothermal synthesis of zeolites history and development from the earliest days to the present time. *Chem. Rev.* **2003**, *103*, 663–701. [CrossRef] [PubMed]
7. Sadrameli, S.M. Thermal/catalytic cracking of liquid hydrocarbons for the production of olefins: A state-of-the-art review II: Catalytic cracking review. *Fuel* **2016**, *173*, 285–297. [CrossRef]
8. Blasco, T.; Corma, A. Martineztriguero, J. Hydrothermal stabilization of ZSM-5 catalytic-cracking additives by phosphorus addition. *J. Catal.* **2006**, *237*, 267–277. [CrossRef]
9. Xue, N.; Nie, L.; Fang, D.; Guo, X.; Shen, J.; Ding, W.; Chen, Y. Synergistic effects of tungsten and phosphorus on catalytic cracking of butene to propene over HZSM-5. *Appl. Catal. A* **2009**, *352*, 87–94. [CrossRef]
10. Luo, J.; Bhaskar, B.V.; Yeh, Y.-H.; Gorte, R.J. n-Hexane cracking at high pressures on H-ZSM-5, H-BEA, H-MOR, and USY for endothermic reforming. *Appl. Catal. A* **2014**, *478*, 228–233. [CrossRef]
11. Pagis, C.; Morgado Prates, A.R.; Farrusseng, D.; Bats, N.; Tuel, A. Hollow Zeolite Structures: An Overview of Synthesis Methods. *Chem. Mater.* **2016**, *28*, 5205–5223. [CrossRef]
12. Choi, M.; Na, K.; Kim, J.; Sakamoto, Y.; Terasaki, O.; Ryoo, R. Stable single-unit-cell nanosheets of zeolite MFI as active and long-lived catalysts. *Nature* **2009**, *461*, 246–249. [CrossRef] [PubMed]
13. Perez-Ramirez, J.; Christensen, C.H.; Egeblad, K.; Christensen, C.H.; Groen, J.C. Hierarchical zeolites: Enhanced utilisation of microporous crystals in catalysis by advances in materials design. *Chem. Soc. Rev.* **2008**, *37*, 2530–2542. [CrossRef] [PubMed]
14. Chal, R.; Gérardin, C.; Bulut, M.; Van Donk, S. Overview and industrial assessment of synthesis strategies towards zeolites with mesopores. *ChemCatChem* **2011**, *3*, 67–81. [CrossRef]
15. Mintova, S.; Jaber, M.; Valtchev, V. Nanosized microporous crystals: Emerging applications. *Chem. Soc. Rev.* **2015**, *44*, 7207–7233. [CrossRef] [PubMed]
16. Rahimi, N.; Karimzadeh, R. Catalytic cracking of hydrocarbons over modified ZSM-5 zeolites to produce light olefins: A review. *Appl. Catal. A* **2011**, *398*, 1–17. [CrossRef]
17. Tao, H.; Li, C.; Ren, J.; Wang, Y.; Lu, G. Synthesis of mesoporous zeolite single crystals with cheap porogens. *J. Solid State Chem.* **2011**, *184*, 1820–1827. [CrossRef]
18. Yin, C.; Wei, Y.; Wang, F.; Chen, Y. Introduction of mesopority in zeolite ZSM-5 using resin as templates. *Mater. Lett.* **2013**, *98*, 194–196. [CrossRef]
19. Garcia-Martinez, J.; Xiao, C.; Cychosz, K.A.; Li, K.; Wan, W.; Zou, X.; Thommes, M. Evidence of Intracrystalline Mesostructured Porosity in Zeolites by Advanced Gas Sorption, Electron Tomography and Rotation Electron Diffraction. *ChemCatChem* **2014**, *6*, 3110–3115. [CrossRef]
20. Mei, C.; Liu, Z.; Wen, P.; Xie, Z.; Hua, W.; Gao, Z. Regular HZSM-5 microboxes prepared via a mild alkaline treatment. *J. Mater. Chem.* **2008**, *18*, 3496–3500. [CrossRef]
21. Fodor, D.; Krumeich, F.; Hauert, R.; Van Bokhoven, J.A. Differences between individual ZSM-5 crystals in forming hollow single crystals and mesopores during base leaching. *Chemistry* **2015**, *21*, 6272–6277. [CrossRef] [PubMed]

22. Dai, C.; Zhang, A.; Liu, M.; Guo, X.; Song, C. Hollow ZSM-5 with Silicon-Rich Surface, Double Shells, and Functionalized Interior with Metallic Nanoparticles and Carbon Nanotubes. *Adv. Funct. Mater.* **2015**, *25*, 7479–7487. [CrossRef]
23. Li, H.; He, S.; Ma, K.; Wu, Q.; Jiao, Q.; Sun, K. Micro-mesoporous composite molecular sieves H-ZSM-5/MCM-41 for methanol dehydration to dimethyl ether: Effect of SiO2/Al2O3 ratio in H-ZSM-5. *Appl. Catal. A* **2013**, *450*, 152–159. [CrossRef]
24. Sang, Y.; Jiao, Q.; Li, H.; Wu, Q.; Zhao, Y.; Sun, K. HZSM-5/MCM-41 composite molecular sieves for the catalytic cracking of endothermic hydrocarbon fuels: Nano-ZSM-5 zeolites as the source. *J. Nanopart. Res.* **2014**, *16*, 2755–2765. [CrossRef]
25. Peng, P.; Wang, Y.; Zhang, Z.; Qiao, K.; Liu, X.; Yan, Z.; Subhan, F.; Komarneni, S. ZSM-5-based mesostructures by combined alkali dissolution and re-assembly: Process controlling and scale-up. *Chem. Eng. J.* **2016**, *302*, 323–333. [CrossRef]
26. Diao, Z.; Wang, L.; Zhang, X.; Liu, G. Catalytic cracking of supercritical n-dodecane over meso-HZSM-5@Al-MCM-41 zeolites. *Chem. Eng. Sci.* **2015**, *135*, 452–460. [CrossRef]
27. Wang, D.; Xu, L.; Wu, P. Hierarchical, core–shell meso-ZSM-5@mesoporous aluminosilicate-supported Pt nanoparticles for bifunctional hydrocracking. *J. Mater. Chem. A* **2014**, *2*, 15535–15545. [CrossRef]
28. Zheng, J.; Wang, G.; Pan, M.; Guo, D.; Zhao, Q.; Li, B.; Li, R. Hierarchical core–shell zeolite composite ZSM-5@SAPO-34 fabricated by using ZSM-5 as the nutrients for the growth of SAPO-34. *Microporous Mesoporous Mater.* **2015**, *206*, 114–120. [CrossRef]
29. Vu, X.H.; Nguyen, S.; Dang, T.T.; Phan, B.M.Q.; Nguyen, D.A.; Armbruster, U.; Martin, A. Catalytic Cracking of Triglyceride-Rich Biomass toward Lower Olefins over a Nano-ZSM-5/SBA-15 Analog Composite. *Catalysts* **2015**, *5*, 1692–1703. [CrossRef]
30. Jiang, J.; Yang, Y.; Duanmu, C.; Xu, Y.; Feng, L.; Gu, X.; Chen, J. Preparation of hollow ZSM-5 crystals in the presence of polyacrylamide. *Microporous Mesoporous Mater.* **2012**, *163*, 11–20. [CrossRef]
31. Tao, H.; Ren, J.; Liu, X.; Wang, Y.; Lu, G. Facile synthesis of hollow zeolite microspheres through dissolution–recrystallization procedure in the presence of organosilanes. *J. Solid State Chem.* **2013**, *200*, 179–188. [CrossRef]
32. Pashkova, V.; Tokarova, V.; Brabec, L.; Dedecek, J. Self-templating synthesis of hollow spheres of zeolite ZSM-5 from spray-dried aluminosilicate precursor. *Microporous Mesoporous Mater.* **2016**, *228*, 59–63. [CrossRef]
33. Groen, J.C.; Bach, T.; Ziese, U.; Donk, A.M.P.-V.; Jong, K.P.D.; Moulijn, J.A.; Pérez-Ramírez, J. Creation of Hollow Zeolite Architectures by Controlled Desilication of Al-Zoned ZSM-5 Crystals. *J. Am. Chem. Soc.* **2005**, *127*, 10792–10793. [CrossRef] [PubMed]
34. Vu, X.; Armbruster, U.; Martin, A. Micro/Mesoporous Zeolitic Composites: Recent Developments in Synthesis and Catalytic Applications. *Catalysts* **2016**, *6*, 183. [CrossRef]
35. Li, G.; Diao, Z.; Na, J.; Wang, L. Exploring suitable ZSM-5/MCM-41 zeolites for catalytic cracking of n-dodecane: Effect of initial particle size and Si/Al ratio. *Chin. J. Chem. Eng.* **2015**, *23*, 1655–1661. [CrossRef]
36. Boukoussa, B.; Aouad, N.; Hamacha, R.; Bengueddach, A. Key factor affecting the structural and textural properties of ZSM-5/MCM-41 composite. *J. Phys. Chem. Solids* **2015**, *78*, 78–83. [CrossRef]
37. Xue, H.; He, Z.; Zhao, Y.; Jiao, Q.; Wu, Q.; Li, H. Controllable synthesis of composites of ZSM-5 and KIT-1 using an ionic liquid as template. *Solid State Sci.* **2017**, *64*, 29–33. [CrossRef]
38. Ghorbanpour, A.; Gumidyala, A.; Grabow, L.C.; Crossley, S.P.; Rime, J.D. Epitaxial Growth of ZSM-5@Silicalite-1: A Core-Shell Zeolite Designed with Passivated Surface Acidity. *ACS Nano* **2015**, *9*, 4006–4016. [CrossRef] [PubMed]
39. Li, N.; Zhang, Y.-Y.; Chen, L.; Au, C.-T.; Yin, S.-F. Synthesis and application of HZSM-5@silicalite-1 core–shell composites for the generation of light olefins from CH3Br. *Microporous Mesoporous Mater.* **2016**, *227*, 76–80. [CrossRef]
40. Vu, X.H.; Bentrup, U.; Hunger, M.; Kraehnert, R.; Armbruster, U.; Martin, A. Direct synthesis of nanosized-ZSM-5/SBA-15 analog composites from preformed ZSM-5 precursors for improved catalytic performance as cracking catalyst. *J. Mater. Sci.* **2014**, *49*, 5676–5689. [CrossRef]
41. Zhu, X.; Wu, L.; Magusin, P.C.M.M.; Mezari, B.; Hensen, E.J.M. On the synthesis of highly acidic nanolayered ZSM-5. *J. Catal.* **2015**, *327*, 10–21. [CrossRef]

42. Xu, D.; Ma, Y.; Jing, Z.; Han, L.; Singh, B.; Feng, J.; Shen, X.; Cao, F.; Oleynikov, P.; Sun, H.; et al. π-π interaction of aromatic groups in amphiphilic molecules directing for single-crystalline mesostructured zeolite nanosheets. *Nat. Commun.* **2014**, *5*, 4262–4270. [CrossRef] [PubMed]
43. Keoh, S.H.; Chaikittisilp, W.; Muraoka, K.; Mukti, R.R.; Shimojima, A.; Kumar, P.; Tsapatsis, M.; Okubo, T. Factors Governing the Formation of Hierarchically and Sequentially Intergrown MFI Zeolites by Using Simple Diquaternary Ammonium Structure-Directing Agents. *Chem. Mater.* **2016**, *28*, 8997–9007. [CrossRef]
44. Ji, Y.; Shi, B.; Yang, H.; Yan, W. Synthesis of isomorphous MFI nanosheet zeolites for supercritical catalytic cracking of n-dodecane. *Appl. Catal. A* **2017**, *533*, 90–98. [CrossRef]
45. Emdadi, L.; Wu, Y.; Zhu, G.; Chang, C.-C.; Fan, W.; Pham, T.; Lobo, R.F.; Liu, D. Dual Template Synthesis of Meso- and Microporous MFI Zeolite Nanosheet Assemblies with Tailored Activity in Catalytic Reactions. *Chem. Mater.* **2014**, *26*, 1345–1355. [CrossRef]
46. Zhang, X.; Liu, D.; Xu, D.; Asahina, S.; Cychosz, K.A.; Agrawal, K.V.; Al Wahedi, Y.; Bhan, A.; Al Hashimi, S.; Terasaki, O.; et al. Synthesis of self-pillared zeolite nanosheets by repetitive branching. *Science* **2012**, *336*, 1684–1687. [CrossRef] [PubMed]
47. Rani, P.; Srivastava, R.; Satpati, B. One-Step Dual Template Mediated Synthesis of Nanocrystalline Zeolites of Different Framework Structures. *Cryst. Growth Des.* **2016**, *16*, 3323–3333. [CrossRef]
48. Kim, J.; Kim, W.; Seo, Y.; Kim, J.-C.; Ryoo, R. n-Heptane hydroisomerization over Pt/MFI zeolite nanosheets: Effects of zeolite crystal thickness and platinum location. *J. Catal.* **2013**, *301*, 187–197. [CrossRef]
49. Park, W.; Yu, D.; Na, K.; Jelfs, K.E.; Slater, B.; Sakamoto, Y.; Ryoo, R. Hierarchically Structure-Directing Effect of Multi-Ammonium Surfactants for the Generation of MFI Zeolite Nanosheets. *Chem. Mater.* **2011**, *23*, 5131–5137. [CrossRef]
50. Na, K.; Jo, C.; Kim, J.; Cho, K.; Jung, J.; Seo, Y.; Messinger, R.J.; Chmelka, B.F.; Ryoo, R. Directing zeolite structures into hierarchically nanoporous architectures. *Science* **2011**, *333*, 328–332. [CrossRef] [PubMed]
51. Koekkoek, A.J.J.; Kim, W.; Degirmenci, V.; Xin, H.; Ryoo, R.; Hensen, E.J.M. Catalytic performance of sheet-like Fe/ZSM-5 zeolites for the selective oxidation of benzene with nitrous oxide. *J. Catal.* **2013**, *299*, 81–89. [CrossRef]
52. Jo, C.; Cho, K.; Kim, J.; Ryoo, R. MFI zeolite nanosponges possessing uniform mesopores generated by bulk crystal seeding in the hierarchical surfactant-directed synthesis. *Chem. Commun.* **2014**, *50*, 4175–4177. [CrossRef] [PubMed]
53. Liu, B.; Zheng, L.; Zhu, Z.; Zhang, K.; Xi, H.; Qian, Y. Effect of synthesis conditions on the structural and catalytic properties of hierarchically structured ZSM-5 zeolites. *RSC Adv.* **2014**, *4*, 13831–13838. [CrossRef]
54. Wu, L.; Magusin, P.C.M.M.; Degirmenci, V.; Li, M.; Almutairi, S.M.T.; Zhu, X.; Mezari, B.; Hensen, E.J.M. Acidic properties of nanolayered ZSM-5 zeolites. *Microporous Mesoporous Mater.* **2014**, *189*, 144–157. [CrossRef]
55. Li, C.; Ren, Y.; Gou, J.; Liu, B.; Xi, H. Facile synthesis of mesostructured ZSM-5 zeolite with enhanced mass transport and catalytic performances. *Appl. Surf. Sci.* **2017**, *392*, 785–794. [CrossRef]
56. Peral, A.; Escola, J.M.; Serrano, D.P.; Přech, J.; Ochoa-Hernández, C.; Čejka, J. Bidimensional ZSM-5 zeolites probed as catalysts for polyethylene cracking. *Catal. Sci. Technol.* **2016**, *6*, 2754–2765. [CrossRef]
57. Ji, M.; Liu, G.; Wang, L.; Zhang, X. Layer by layer fabrication of b-oriented HZSM-5 coatings for supercritical catalytic cracking of *n*-dodecane. *Fuel* **2014**, *134*, 180–188. [CrossRef]
58. Ji, M.; Liu, G.; Chen, C.; Wang, L.; Zhang, X.; Hu, S.; Ma, X. Catalytic performances of b-oriented bi-layered HZSM-5 coatings for cracking of hydrocarbon fuels. *Appl. Catal. A* **2014**, *482*, 8–15. [CrossRef]
59. Peng, Y.; Lu, X.; Wang, Z.; Yan, Y. Fabrication of b-Oriented MFI Zeolite Films under Neutral Conditions without the Use of Hydrogen Fluoride. *Angew. Chem. Int. Ed. Engl.* **2015**, *54*, 5709–5712. [CrossRef] [PubMed]
60. Lu, X.; Peng, Y.; Wang, Z.; Yan, Y. Rapid fabrication of highly b-oriented zeolite MFI thin films using ammonium salts as crystallization-mediating agents. *Chem. Commun.* **2015**, *51*, 11076–11079. [CrossRef] [PubMed]
61. Lu, X.; Peng, Y.; Wang, Z.; Yan, Y. A facile fabrication of highly b-oriented MFI zeolite films in the TEOS-TPAOH-H2O system without additives. *Microporous Mesoporous Mater.* **2016**, *230*, 49–57. [CrossRef]

62. Zheng, J.; Zhang, H.; Liu, Y.; Wang, G.; Kong, Q.; Pan, M.; Tian, H.; Li, R. Synthesis of Wool-Ball-Like ZSM-5 with Enlarged External Surfaces and Improved Diffusion: A Potential Highly-Efficient FCC Catalyst Component for Elevating Pre-cracking of Large Molecules and Catalytic Longevity. *Catal. Lett.* **2016**, *146*, 1457–1469. [CrossRef]
63. Firmansyah, M.L.; Jalil, A.A.; Triwahyono, S.; Hamdan, H.; Salleh, M.M.; Ahmad, W.F.W.; Kadja, G.T.M. Synthesis and characterization of fibrous silica ZSM-5 for cumene hydrocracking. *Catal. Sci. Technol.* **2016**, *6*, 5178–5182. [CrossRef]
64. Liu, J.; Jiang, G.; Liu, Y.; Di, J.; Wang, Y.; Zhao, Z.; Sun, Q.; Xu, C.; Gao, J.; Duan, A.; et al. Hierarchical macro-meso-microporous ZSM-5 zeolite hollow fibers with highly efficient catalytic cracking capability. *Sci. Rep.* **2014**, *4*, 7276–7281. [CrossRef] [PubMed]
65. Han, J.; Jiang, G.; Han, S.; Liu, J.; Zhang, Y.; Liu, Y.; Wang, R.; Zhao, Z.; Xu, C.; Wang, Y.; et al. The Fabrication of Ga_2O_3/ZSM-5 Hollow Fibers for Efficient Catalytic Conversion of n-Butane into Light Olefins and Aromatics. *Catalysts* **2016**, *6*, 13. [CrossRef]
66. Fu, T.; Zhou, H.; Li, Z. Effect of Particle Morphology for ZSM-5 Zeolite on the Catalytic Conversion of Methanol to Gasoline-Range Hydrocarbons. *Catal. Lett.* **2016**, *146*, 1973–1983. [CrossRef]
67. Zhang, K.; Ostraat, M.L. Innovations in hierarchical zeolite synthesis. *Catal. Today* **2016**, *264*, 3–15. [CrossRef]
68. Chen, L.; Li, X.; Rooke, J.C.; Zhang, Y.; Yang, X.; Tang, Y.; Xiao, F.; Su, B. Hierarchically structured zeolites: Synthesis, mass transport properties and applications. *J. Mater. Chem.* **2012**, *22*, 17381–17403. [CrossRef]
69. Zhang, L.; Qu, S.; Wang, L.; Zhang, X.; Liu, G. Preparation and performance of hierarchical HZSM-5 coatings on stainless-steeled microchannels for catalytic cracking of hydrocarbons. *Catal. Today* **2013**, *216*, 64–70. [CrossRef]
70. Miyake, K.; Hirota, Y.; Uchida, Y.; Nishiyama, N. Synthesis of mesoporous MFI zeolite using PVA as a secondary template. *J. Porous Mater.* **2016**, *23*, 1395–1399. [CrossRef]
71. Qiu, Y.; Wang, L.; Zhang, X.; Liu, G. Different roles of CNTs in hierarchical HZSM-5 synthesis with hydrothermal and steam-assisted crystallization. *RSC Adv.* **2015**, *5*, 78238–78246. [CrossRef]
72. Bai, P.; Wu, P.; Xing, W.; Liu, D.; Zhao, L.; Wang, Y.; Xu, B.; Yan, Z.; Zhao, X.S. Synthesis and catalytic properties of ZSM-5 zeolite with hierarchical pores prepared in the presence of *n*-hexyltrimethylammonium bromide. *J. Mater. Chem. A* **2015**, *3*, 18586–18597. [CrossRef]
73. Xue, T.; Liu, H.; Zhang, Y.; Wu, H.; Wu, P.; He, M. Synthesis of ZSM-5 with hierarchical porosity: In-situ conversion of the mesoporous silica-alumina species to hierarchical zeolite. *Microporous Mesoporous Mater.* **2017**, *242*, 190–199. [CrossRef]
74. Ding, J.; Hu, J.; Xue, T.; Wang, Y.; Wu, H.; Wu, P.; He, M. Direct synthesis of self-assembled ZSM-5 microsphere with controllable mesoporosity and its enhanced LDPE cracking properties. *RSC Adv.* **2016**, *6*, 38671–38679. [CrossRef]
75. Wan, Z.; Wu, W.; Chen, W.; Yang, H.; Zhang, D. Direct Synthesis of Hierarchical ZSM-5 Zeolite and Its Performance in Catalyzing Methanol to Gasoline Conversion. *Ind. Eng. Chem. Res.* **2014**, *53*, 19471–19478. [CrossRef]
76. Ge, T.; Hua, Z.; He, X.; Zhu, Y.; Ren, W.; Chen, L.; Zhang, L.; Chen, H.; Lin, C.; Yao, H.; et al. One-pot synthesis of hierarchically structured ZSM-5 zeolites using single micropore-template. *Chin. J. Catal.* **2015**, *36*, 866–873. [CrossRef]
77. Zhang, X.; Wang, R.; Yang, X. Effect of alkaline treatment on pore structure and acidity of HZSM-5 in the synthesis of ethyl mercaptan. *Catal. Commun.* **2015**, *60*, 32–36. [CrossRef]
78. Shahid, A.; Lopez-Orozco, S.; Marthala, V.R.; Hartmann, M.; Schwieger, W. Direct oxidation of benzene to phenol over hierarchical ZSM-5 zeolites prepared by sequential post synthesis modification. *Microporous Mesoporous Mater.* **2017**, *237*, 151–159. [CrossRef]
79. Shahid, A.; Ahmed, N.; Saleh, T.; Al-Thabaiti, S.; Basahel, S.; Schwieger, W.; Mokhtar, M. Solvent-Free Biginelli Reactions Catalyzed by Hierarchical Zeolite Utilizing a Ball Mill Technique: A Green Sustainable Process. *Catalysts* **2017**, *7*, 84. [CrossRef]
80. Wang, D.; Zhang, L.; Chen, L.; Wu, H.; Wu, P. Postsynthesis of mesoporous ZSM-5 zeolite by piperidine-assisted desilication and its superior catalytic properties in hydrocarbon cracking. *J. Mater. Chem. A* **2015**, *3*, 3511–3521. [CrossRef]
81. Nandan, D.; Saxena, S.K.; Viswanadham, N. Synthesis of hierarchical ZSM-5 using glucose as a templating precursor. *J. Mater. Chem. A* **2014**, *2*, 1054–1059. [CrossRef]

82. Deng, Z.; Zhang, Y.; Zhu, K.; Qian, G.; Zhou, X. Carbon nanotubes as transient inhibitors in steam-assisted crystallization of hierarchical ZSM-5 zeolites. *Mater. Lett.* **2015**, *159*, 466–469. [CrossRef]
83. Han, S.; Wang, Z.; Meng, L.; Jiang, N. Synthesis of uniform mesoporous ZSM-5 using hydrophilic carbon as a hard template. *Mater. Chem. Phys.* **2016**, *177*, 112–117. [CrossRef]
84. Liu, Z.; Wu, D.; Ren, S.; Chen, X.; Qiu, M.; Liu, G.; Zeng, G.; Sun, Y. Facile one-pot solvent-free synthesis of hierarchical ZSM-5 for methanol to gasoline conversion. *RSC Adv.* **2016**, *6*, 15816–15820. [CrossRef]
85. Choi, M.; Cho, H.S.; Srivastava, R.; Venkatesan, C.; Choi, D.-H.; Ryoo, R. Amphiphilic organosilane-directed synthesis of crystalline zeolite with tunable mesoporosity. *Nat. Mater.* **2006**, *5*, 718–723. [CrossRef] [PubMed]
86. Zhu, X.; Rohling, R.; Filonenko, G.; Mezari, B.; Hofmann, J.P.; Asahina, S.; Hensen, E.J. Synthesis of hierarchical zeolites using an inexpensive mono-quaternary ammonium surfactant as mesoporogen. *Chem. Commun.* **2014**, *50*, 14658–14661. [CrossRef] [PubMed]
87. Wang, X.; Gao, X.; Dong, M.; Zhao, H.; Huang, W. Production of gasoline range hydrocarbons from methanol on hierarchical ZSM-5 and Zn/ZSM-5 catalyst prepared with soft second template. *J. Energy Chem.* **2015**, *24*, 490–496. [CrossRef]
88. Zhou, F.; Gao, Y.; Wu, G.; Ma, F.; Liu, C. Improved catalytic performance and decreased coke formation in post-treated ZSM-5 zeolites for methanol aromatization. *Microporous Mesoporous Mater.* **2017**, *240*, 96–107. [CrossRef]
89. Xiao, W.; Wang, F.; Xiao, G. Performance of hierarchical HZSM-5 zeolites prepared by NaOH treatments in the aromatization of glycerol. *RSC Adv.* **2015**, *5*, 63697–63704. [CrossRef]
90. Mochizuki, H.; Yokoi, T.; Imai, H.; Namba, S.; Kondo, J.N.; Tatsumi, T. Effect of desilication of H-ZSM-5 by alkali treatment on catalytic performance in hexane cracking. *Appl. Catal. A* **2012**, *449*, 188–197. [CrossRef]
91. Groen, J.C.; Moulijn, J.A.; Pérez-Ramírez, J. Desilication: On the controlled generation of mesoporosity in MFI zeolites. *J. Mater. Chem.* **2006**, *16*, 2121–2131. [CrossRef]
92. Yuan, E.; Tang, Z.; Mo, Z.; Lu, G. A new method to construct hierarchical ZSM-5 zeolites with excellent catalytic activity. *J. Porous Mater.* **2014**, *21*, 957–965. [CrossRef]
93. Abelló, S.; Bonilla, A.; Pérez-Ramírez, J. Mesoporous ZSM-5 zeolite catalysts prepared by desilication with organic hydroxides and comparison with NaOH leaching. *Appl. Catal. A* **2009**, *364*, 191–198. [CrossRef]
94. Meng, F.; Wang, Y.; Wang, S. Methanol to gasoline over zeolite ZSM-5: Improved catalyst performance by treatment with HF. *RSC Adv.* **2016**, *6*, 58586–58593. [CrossRef]
95. Qin, Z.; Lakiss, L.; Gilson, J.P.; Thomas, K.; Goupil, J.M.; Fernandez, C.; Valtchev, V. Chemical Equilibrium Controlled Etching of MFI-Type Zeolite and Its Influence on Zeolite Structure, Acidity, and Catalytic Activity. *Chem. Mater.* **2013**, *25*, 2759–2766. [CrossRef]
96. Qin, Z.; Gilson, J.-P.; Valtchev, V. Mesoporous zeolites by fluoride etching. *Curr. Opin. Chem. Eng.* **2015**, *8*, 1–6. [CrossRef]
97. Li, M.; Zhou, Y.; Ju, C.; Fang, Y. Remarkable increasing of ZSM-5 lifetime in methanol to hydrocarbon reaction by post engineering in fluoride media. *Appl. Catal. A* **2016**, *512*, 1–8. [CrossRef]
98. Mochizuki, H.; Yokoi, T.; Imai, H.; Watanabe, R.; Namba, S.; Kondo, J.N.; Tatsumi, T. Facile control of crystallite size of ZSM-5 catalyst for cracking of hexane. *Microporous Mesoporous Mater.* **2011**, *145*, 165–171. [CrossRef]
99. Popov, A.G.; Pavlov, V.S.; Ivanova, I.I. Effect of crystal size on butenes oligomerization over MFI catalysts. *J. Catal.* **2016**, *335*, 155–164. [CrossRef]
100. Alipour, S.M. Recent advances in naphtha catalytic cracking by nano ZSM-5: A review. *Chin. J. Catal.* **2016**, *37*, 671–680. [CrossRef]
101. Konno, H.; Tago, T.; Nakasaka, Y.; Ohnaka, R.; Nishimura, J.-I.; Masuda, T. Effectiveness of nano-scale ZSM-5 zeolite and its deactivation mechanism on catalytic cracking of representative hydrocarbons of naphtha. *Microporous Mesoporous Mater.* **2013**, *175*, 25–33. [CrossRef]
102. Nakasaka, Y.; Okamura, T.; Konno, H.; Tago, T.; Masuda, T. Crystal size of MFI-type zeolites for catalytic cracking of n-hexane under reaction-control conditions. *Microporous Mesoporous Mater.* **2013**, *182*, 244–249. [CrossRef]
103. Javaid, R.; Urata, K.; Furukawa, S.; Komatsu, T. Factors affecting coke formation on H-ZSM-5 in naphtha cracking. *Appl. Catal. A* **2015**, *491*, 100–105. [CrossRef]

104. Lakiss, L.; Ngoye, F.; Canaff, C.; Laforge, S.; Pouilloux, Y.; Qin, Z.; Tarighi, M.; Thomas, K.; Valtchev, V.; Vicente, A.; et al. On the remarkable resistance to coke formation of nanometer-sized and hierarchical MFI zeolites during ethanol to hydrocarbons transformation. *J. Catal.* **2015**, *328*, 165–172. [CrossRef]
105. Chen, H.; Wang, Y.; Meng, F.; Li, H.; Wang, S.; Sun, C.; Wang, S.; Wang, X. Conversion of methanol to propylene over nano-sized ZSM-5 zeolite aggregates synthesized by a modified seed-induced method with CTAB. *RSC Adv.* **2016**, *6*, 76642–76651. [CrossRef]
106. Kang, N.Y.; Woo, S.I.; Lee, Y.J.; Bae, J.; Choi, W.C.; Park, Y.-K. Enhanced hydrothermal stability of ZSM-5 formed from nanocrystalline seeds for naphtha catalytic cracking. *J. Mater. Sci.* **2016**, *51*, 3735–3749. [CrossRef]
107. Shi, L.; Wang, J.; Li, N.; Lin, S. Direct synthesis of monolithic nano-sized ZSM-5 aggregates possessing ordered mesoporosity by controlling arrangement of nanoparticles. *J. Alloys Compd.* **2017**, *695*, 2488–2498. [CrossRef]
108. Wakihara, T.; Sato, K.; Inagaki, S.; Tatami, J.; Komeya, K.; Meguro, T.; Kubota, Y. Fabrication of Fine Zeolite with Improved Catalytic Properties by Bead Milling and Alkali Treatment. *ACS Appl. Mater. Interfaces* **2010**, *2*, 2715–2718. [CrossRef]
109. Rosilda, S.T.; Chiang, A.S. Some Observations on the Synthesis of Fully-Dispersible Nanocrystalline Zeolite ZSM-5. *J. Nanosci. Nanotechnol.* **2014**, *14*, 7351–7359.
110. Nada, M.H.; Larsen, S.C. Insight into seed-assisted template free synthesis of ZSM-5 zeolites. *Microporous Mesoporous Mater.* **2017**, *239*, 444–452. [CrossRef]
111. Inagaki, S.; Shinoda, S.; Hayashi, S.; Wakihara, T.; Yamazaki, H.; Kondo, J.N.; Kubota, Y. Improvement in the catalytic properties of ZSM-5 zeolite nanoparticles via mechanochemical and chemical modifications. *Catal. Sci. Technol.* **2016**, *6*, 2598–2604. [CrossRef]
112. Lin, L.F.; Zhao, S.F.; Zhang, D.W.; Fan, H.; Liu, Y.M.; He, M.Y. Acid Strength Controlled Reaction Pathways for the Catalytic Cracking of 1-Pentene to Propene over ZSM-5. *ACS Catal.* **2015**, *5*, 4048–4059. [CrossRef]
113. Hodoshima, S.; Motomiya, A.; Wakamatsu, S.; Kanai, R.; Yagi, F. Catalytic conversion of light hydrocarbons to propylene over MFI-zeolite/metal-oxide composites. *Microporous Mesoporous Mater.* **2016**, *233*, 125–132. [CrossRef]
114. Furumoto, Y.; Harada, Y.; Tsunoji, N.; Takahashi, A.; Fujitani, T.; Ide, Y.; Sadakane, M.; Sano, T. Effect of acidity of ZSM-5 zeolite on conversion of ethanol to propylene. *Appl. Catal. A* **2011**, *399*, 262–267. [CrossRef]
115. Wan, Z.; Wu, W.; Li, G.; Wang, C.; Yang, H.; Zhang, D. Effect of SiO_2/Al_2O_3 ratio on the performance of nanocrystal ZSM-5 zeolite catalysts in methanol to gasoline conversion. *Appl. Catal. A* **2016**, *523*, 312–320. [CrossRef]
116. Qi, C.; Wang, Y.; Ding, X.; Su, H. Catalytic cracking of light diesel over Au/ZSM-5 catalyst for increasing propylene production. *Chin. J. Catal.* **2016**, *37*, 1747–1754. [CrossRef]
117. Epelde, E.; Santos, J.I.; Florian, P.; Aguayo, A.T.; Gayubo, A.G.; Bilbao, J.; Castaño, P. Controlling coke deactivation and cracking selectivity of MFI zeolite by H3PO4 or KOH modification. *Appl. Catal. A* **2015**, *505*, 105–115. [CrossRef]
118. Ji, Y.; Yang, H.; Zhang, Q.; Yan, W. Phosphorus modification increases catalytic activity and stability of ZSM-5 zeolite on supercritical catalytic cracking of *n*-dodecane. *J. Solid State Chem.* **2017**, *251*, 7–13. [CrossRef]
119. Tsunoji, N.; Sonoda, T.; Furumoto, Y.; Sadakane, M.; Sano, T. Recreation of Brønsted acid sites in phosphorus-modified HZSM-5(Ga) by modification with various metal cations. *Appl. Catal. A* **2014**, *481*, 161–168. [CrossRef]
120. Lee, J.; Hong, U.G.; Hwang, S.; Youn, M.H.; Song, I.K. Catalytic cracking of C5 raffinate to light olefins over lanthanum-containing phosphorous-modified porous ZSM-5: Effect of lanthanum content. *Fuel Process. Technol.* **2013**, *109*, 189–195. [CrossRef]
121. Rahimi, N.; Moradi, D.; Sheibak, M.; Moosavi, E.; Karimzadeh, R. The influence of modification methods on the catalytic cracking of LPG over lanthanum and phosphorus modified HZSM-5 catalysts. *Microporous Mesoporous Mater.* **2016**, *234*, 215–223. [CrossRef]
122. Li, J.; Li, T.; Ma, H.; Sun, Q.; Ying, W.; Fang, D. Effect of Impregnating Fe into P-Modified HZSM-5 in the Coupling Cracking of Butene and Pentene. *Ind. Eng. Chem. Res.* **2015**, *54*, 1796–1805. [CrossRef]
123. Li, J.-W.; Li, T.; Ma, H.-F.; Sun, Q.-W.; Ying, W.-Y.; Fang, D.-Y. Effect of nickel on phosphorus modified HZSM-5 in catalytic cracking of butene and pentene. *Fuel Process. Technol.* **2017**, *159*, 31–37. [CrossRef]

124. Inagaki, S.; Shinoda, S.; Kaneko, Y.; Takechi, K.; Komatsu, R.; Tsuboi, Y.; Yamazaki, H.; Kondo, J.N.; Kubota, Y. Facile fabrication of ZSM-5 zeolite catalyst with high durability to coke formation during catalytic cracking of paraffins. *ACS Catal.* **2013**, *3*, 74–78. [CrossRef]
125. Zhang, B.; Zhong, Z.; Xie, Q.; Chen, P.; Ruan, R. Reducing coke formation in the catalytic fast pyrolysis of bio-derived furan with surface modified HZSM-5 catalysts. *RSC Adv.* **2015**, *5*, 56286–56292. [CrossRef]
126. Inagaki, S.; Sato, K.; Hayashi, S.; Tatami, J.; Kubota, Y.; Wakihara, T. Mechanochemical approach for selective deactivation of external surface acidity of ZSM-5 zeolite catalyst. *ACS Appl. Mater. Interfaces* **2015**, *7*, 4488–4493. [CrossRef] [PubMed]